Corresponding author:
Graham R. Fleming;
Email: grfleming@lbl.gov

The development and applications of multidimensional biomolecular spectroscopy illustrated by photosynthetic light harvesting

Graham R. Fleming[1,2] and Gregory D. Scholes[3]

[1]Department of Chemistry and QB3 Institute, Kavli Energy Nanoscience Institute, University of California, Berkeley, CA, USA; [2]Molecular Biophysics and Integrated Bioimaging Division, Lawrence Berkeley National Laboratory, Berkeley, CA, USA and [3]Department of Chemistry, Princeton University, Princeton, NJ, USA

Abstract

The parallel and synergistic developments of atomic resolution structural information, new spectroscopic methods, their underpinning formalism, and the application of sophisticated theoretical methods have led to a step function change in our understanding of photosynthetic light harvesting, the process by which photosynthetic organisms collect solar energy and supply it to their reaction centers to initiate the chemistry of photosynthesis. The new spectroscopic methods, in particular multidimensional spectroscopies, have enabled a transition from recording rates of processes to focusing on mechanism. We discuss two ultrafast spectroscopies – two-dimensional electronic spectroscopy and two-dimensional electronic-vibrational spectroscopy – and illustrate their development through the lens of photosynthetic light harvesting. Both spectroscopies provide enhanced spectral resolution and, in different ways, reveal pathways of energy flow and coherent oscillations which relate to the quantum mechanical mixing of, for example, electronic excitations (excitons) and nuclear motions. The new types of information present in these spectra provoked the application of sophisticated quantum dynamical theories to describe the temporal evolution of the spectra and provide new questions for experimental investigation. While multidimensional spectroscopies have applications in many other areas of science, we feel that the investigation of photosynthetic light harvesting has had the largest influence on the development of spectroscopic and theoretical methods for the study of quantum dynamics in biology, hence the focus of this review. We conclude with key questions for the next decade of this review.

Table of contents

CAMBRIDGE
UNIVERSITY PRESS

Introduction

Photosynthetic light harvesting in nature has had the most impact on the development of spectroscopic and theoretical methods for the study of quantum dynamics in biology. Why and how did biology, physical chemistry, and physics collide in the study of mechanisms of light harvesting in photosynthesis?

Light harvesting is used in photosynthesis to amplify the photoexcitation rate of enzymes known as photosystems, or reaction centers (RCs; Björn and Govindjee, 2009; Mirkovic *et al.*, 2017; Blankenship, 2021). A photoexcitation rate more than a hundred times than that possible with direct excitation of the RCs is needed to ratchet the enzymes through a sequence of intermediate states faster than competing back reactions. This is achieved by flanking the photosystems with chromophore-dense proteins known as light-harvesting complexes (LHCs;

Croce and van Amerongen, 2014). The LHCs play secondary, but important, roles in regulating the delivery of excitation to the RCs under variable light conditions. A detailed review of light harvesting in photosynthesis, including the historical development of our understanding, is found in Mirkovic *et al.* (2017).

LHCs accomplish the amplification of excitation delivery to photosystems by having a large spatial and spectral cross-section for light absorption and using very efficient multistep energy transfer to deliver the excitation to RCs. The transfer of remote excitation to RCs happens with a quantum efficiency of over 90%, despite excitation hopping more than a thousand times on average, chromophore to chromophore, in the excited state lifetime of about 4 ns. What is striking for physical scientists are the detailed and numerous optimizations of energy transfer evident in LHC design – the product of 3 billion years of evolution. In the biological context, it is remarkable that this machinery functions on the 100 fs time-scale (Figure 1).

It further turns out that these natural proteins are remarkable model systems that have enabled step-changes in our understanding of fundamental chemical dynamics with molecular resolution (Scholes *et al.*, 2011), as we describe in this review. Discerning these design principles has required the development of new spectroscopic techniques which, in turn, require improved theoretical methods for their full interpretation. In this review, we will focus on how the rapidly improving knowledge of structures of the membrane-bound pigment–protein complexes and their assembly into larger structures has progressively challenged our experimental and theoretical skill sets and led to widely applicable new methods with applications far beyond photosynthesis.

The reason that photosynthetic light harvesting makes such demands on the experimental and theoretical methods is that nature has settled on a balance of energy scales, where the electronic interaction between the chromophores – which promotes the energy jump – is similar in scale to the interactions between chromophores and the environment – that broadens spectral lines and ensures energy conservation. This infamous 'intermediate regime' of energy transfer is the most difficult to resolve because there is no factor that can be taken as a perturbation. Photosynthetic antennas are generally composed of many chemically identical molecules, such as chlorophyll *a* in plants and green algae, leading to highly congested spectra. This lack, in many cases, of clearly identifiable donor and acceptor bands has pushed the development of spectroscopies with improved spectral resolution without sacrificing the femtosecond time resolution of simple pump–probe methods.

In this review, we focus on light harvesting, and particularly how development of new multidimensional spectroscopic methods enabled a deeper understanding of the underlying physical

mechanisms. There are many other important, related studies that we will not discuss – especially work on electron transfer in photosynthetic RCs. Our goal is not to provide an exhaustive review of the state-of-the-art, but instead, we have attempted to provide examples that show how the field has developed. We use 'boxes' to highlight some of the key scientific questions that motivated experimental and theoretical advances. We end with suggestions of open questions for future work, then discuss what is needed to answer them. While the flavor of the review conveys a personal perspective on how such methods came about, we have endeavored to include key developments from other laboratories. We abbreviate chlorophyll *a* to Chl *a*, chlorophyll *b* to Chl *b*, bacteriochlorophyll *a* to BChl *a*, and so forth. Note that the lowest singlet excited states of Chl and BChl are labeled Q_y and Q_x. The lowest states of carotenoids (also in increasing order of energy) are labeled S_1 (which is a dark state) and S_2.

Beginnings

My thesis advisor, George Porter, had a career-long interest in the photochemical and photophysical aspects of photosynthesis. He said that 'The study of photosynthesis is, and probably always will be, the greatest odyssey of the photochemist' (Fleming and Phillips, 2004). In the mid-1970s, when I was a student at the Royal Institution (RI), the idea of a photosynthetic unit with several hundred antenna chlorophyll (Chl) molecules surrounding a RC with a small number of Chl and pheophytin molecules was well accepted, but debate lingered on as to whether the Chl simply floated in the lipid bilayer of the thylakoid membrane or was bound in protein complexes. By the time I returned to the RI after a brief postdoctoral stay at Cal Tech and a longer one with the same advisor (G. Wilse Robinson) in Melbourne, picosecond resolution experiments were underway at the RI on photosynthetic light harvesting and the potential of ultrafast spectroscopy to unravel the primary steps in photosynthesis was coming into focus.

When I began my independent career at the University of Chicago, the first pigment–protein structure (the FMO complex of green sulfur bacteria (Matthews and Fenna, 1980)) had become available. The structure showed firmly bound BChl molecules with nearest neighbor separations of about 12 Å. Much earlier (in 1950), Arnold and Oppenheimer (1950) had estimated a 10 ps hopping time between Chls in the antenna of photosystem II (PSII), but it was becoming clear, largely from the work of L. Duysens in Leiden (Duysens, 1951), that the elementary steps of energy transfer were much faster than Arnold and Oppenheimer's estimate. By 1964, Duysens (1964) estimated a timescale of 10^{-13} s for an energy transfer step between two Chl. Two years later, in his only paper on photosynthesis, G. W. Robinson discussed a 50 fs exciton
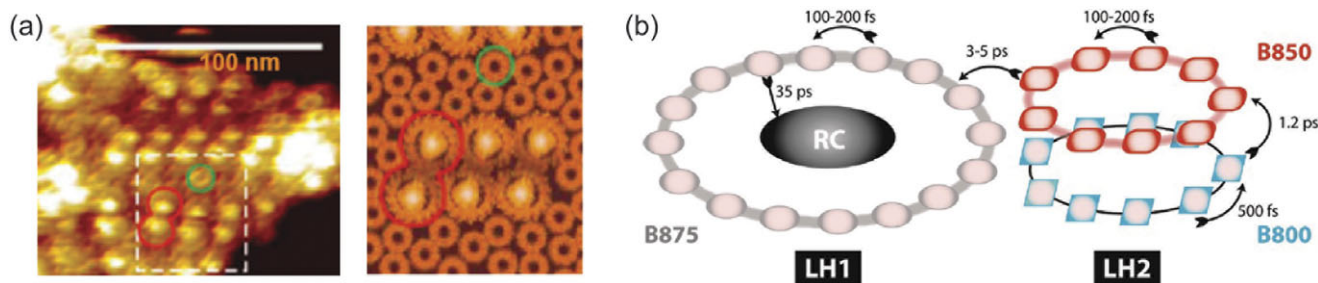
Figure 1. (a) An image (Sturgis *et al.* 2009) of the light-harvesting complexes embedded in the photosynthetic membrane from the purple bacterium *Rb. sphaeroides*. An LH1-reaction center dimer complex is circled in red, an LH2 complex is circled in green. Copyright 2009 American Chemical Society. (b) Schematic of neighboring LH2 and LH1 complexes that shows the timescales of light-harvesting pathways (Fleming and van Grondelle 1997). Reprinted with permission from Elsevier.

'spreading' time, thereby making the first mention of quantum coherence in photosynthetic light harvesting (Robinson, 1966). The questions, preserved in Robinson (1966), made it clear that actually recording events on such a timescale was difficult to imagine, and that 'it may be very difficult to very settle the question of the timescale of exciton motion'. All prior and most subsequent discussions in the 20th century were couched in the incoherent hopping picture of very weak coupling Förster theory, described below.

My department chair when I arrived at Chicago in 1979 was John Light, a theorist and expert in scattering theory in molecular beams. He asked what I planned to do and I mumbled about light harvesting and barrier crossing in solution. John's comment was 'those systems are too messy to learn anything from'. Rather than being discouraging, this comment led to a career-long desire to improve ultrafast spectroscopic methods so that the 'messy' systems of photosynthesis can be understood, and their design principles elucidated as guides for bio-inspired photoconversion devices. I should add that John Light was a supportive chair and colleague throughout my very happy 18 years at the University of Chicago.

Certainly, measuring the timescales and mechanisms of energy flow in the antenna of PSII, for example, seemed a daunting challenge in 1979. In addition to being really, really fast, most of the transfers are between chemically identical molecules, and as Robinson hinted, it might not be a simple rate process. One idea was to use fluorescence polarization as suggested by Arnold and Meek in 1956, and carried out in my lab in 1994 with 90 fs resolution (Du *et al.*, 1994). We found a Chl *b* to Chl *a* transfer time of ~250 fs in the major LHC LHCII, but realized that there were shorter timescales in the data that we were unable to resolve.

Breakthroughs in integral membrane protein structure determination, first with the purple bacterial RC (Deisenhofer and Michel, 2004), then with the LH2 LHC (McDermott *et al.*, 1995; Koepke *et al.*, 1996), enabled key questions such as the nature of the excited states formed by light absorption, the quantum dynamical mechanisms of energy and electron transfer, and whether existing theories were adequate, to come into focus. In parallel, experimental developments, particularly on photon echo methods, suggested ways in which spectral broadening could be defeated or even turned to advantage. Systems-level questions also began to be approachable, such as how light harvesting is regulated in the PSII antenna/RC responsible for water splitting and oxygen evolution. This latter topic is the subject of active research and debate to the current day.

The purple bacterial LH2 complex (Figures 1, 2) proved to be an ideal test bed for many of these ideas and questions. The complex consists of two rings of BChl molecules; a more weakly interacting ring (B800) with eight or nine BChls depending on species, and a second, more strongly coupled, ring of 16 or 18 BChls (B850). The ring names provide the wavelength in nm of the maximum absorption of each ring. The B800 to B850 transfer could easily be measured by simple pump–probe spectroscopy in a manner no different in principle from Porter and Norrish's flash photolysis experiment in 1949. This was first done by Sundström *et al.* (1986), and very precisely by Joo *et al.* (1996) 10 years later when Ti: sapphire laser technology became available. Joo *et al.* (1996) found 800 fs for the timescale of this transfer. We (G.D.S. and G.R.F.) tried to calculate this timescale from standard Förster theory but our calculated rates were always too slow. We began to suspect that the problem lay in treating the process as a one-molecule to one-molecule energy transfer. What if the more strongly coupled B850 BChls had excited states delocalized over two or more BChls? This led G.D.S. and, entirely independently, H. Sumi in Japan to develop generalized Forster theory (GFT), which allows donors or acceptors to be delocalized over more than one molecule (Sumi, 1999; Scholes and Fleming, 2000). Now, the B800 to B850 rate made sense.

Immediately, another problem came up. We could clearly resolve BChl Q_y to carotenoid S_1 electronic energy transfer (EET) (a potential major clue to plant and algal photoprotection), but naïve application of Forster theory suggested this rate should be zero because the S_0 to S_1 optical transition is forbidden in carotenoids, and no dipole–dipole coupling should be possible. However, notice that each molecule is large compared to the distance between their centers, so that there is a lot of 'structure' to the interaction. Therefore, we cannot average over transitions densities – thus removing all this structure – and apply the dipole–dipole coupling approximation. In other words, the way two molecules in close proximity see each other is very different than the way light views a molecule. The light averages over the whole transition density of the carotenoid and detects no net transition dipole. But a BChl (or Chl) molecule close to a carotenoid does not take the average the same way. In the transition density cube (TDC) approach (Krueger *et al.*, 1998), we divided up the transition densities of the donor and acceptor into tiny cubes and explicitly calculated the Coulomb interaction for each pair of cubes (some more detail is given below). The total Coulomb coupling was no longer found to be zero, but we predict a respectable value that easily gave energy transfer rates of 10^{12} s^{-1} (between dipole-forbidden transitions!) as observed (Walla *et al.*, 2000). The TDC has become a standard method of calculating coupling between Chls in photosynthetic complexes.

The third rate we wanted to measure in LH2 was the B850 to B850 transfer rate along with the B875 to B875 rate in the larger LH1 ring that surrounds the RC in purple bacteria. Time and spectrally resolved pump–probe methods would obviously not work in these cases, but maturing photon echo spectroscopic methods suggested a way forward. The photon echo peak shift method records the loss of memory of the initial excitation frequency. Now, inhomogeneous broadening can be turned to advantage as energy transfer around the B850 and B875 rings averages over the site energy distribution and leads directly to the decay of the peak shift (Jimenez *et al.*, 1997). In addition, the method can have very high time resolution. Analysis of the data led to timescales of energy transfer of 90–200 fs for both rings. While the transfer is confined to highly symmetric rings, the analysis is relatively straightforward though it clearly involves interactions more complex than are present in basic Förster theory. However, for the three-dimensional arrays of Chl molecules held in the pigment–protein complexes that comprise the antenna of PSII, the one-dimensional photon echo measurements contain too little information for unambiguous analysis. This led me to develop and apply two-dimensional spectroscopies and shift our focus back to the FMO complex.

In the following sections of the review, we examine this story by establishing the scientific questions at the core and how we needed to address them. Thus the narrative starts with a discussion of EET, the fundamental photophysical process that enables light harvesting.

Electronic energy transfer

Förster theory provides an intuitive and quantitative theory for predicting EET rates when electronic coupling between the energy donor molecule and energy acceptor is very small (Förster, 1965; Scholes, 2003). The equation is cast in terms of experimentally measured quantities: the donor molecule's fluorescence quantum
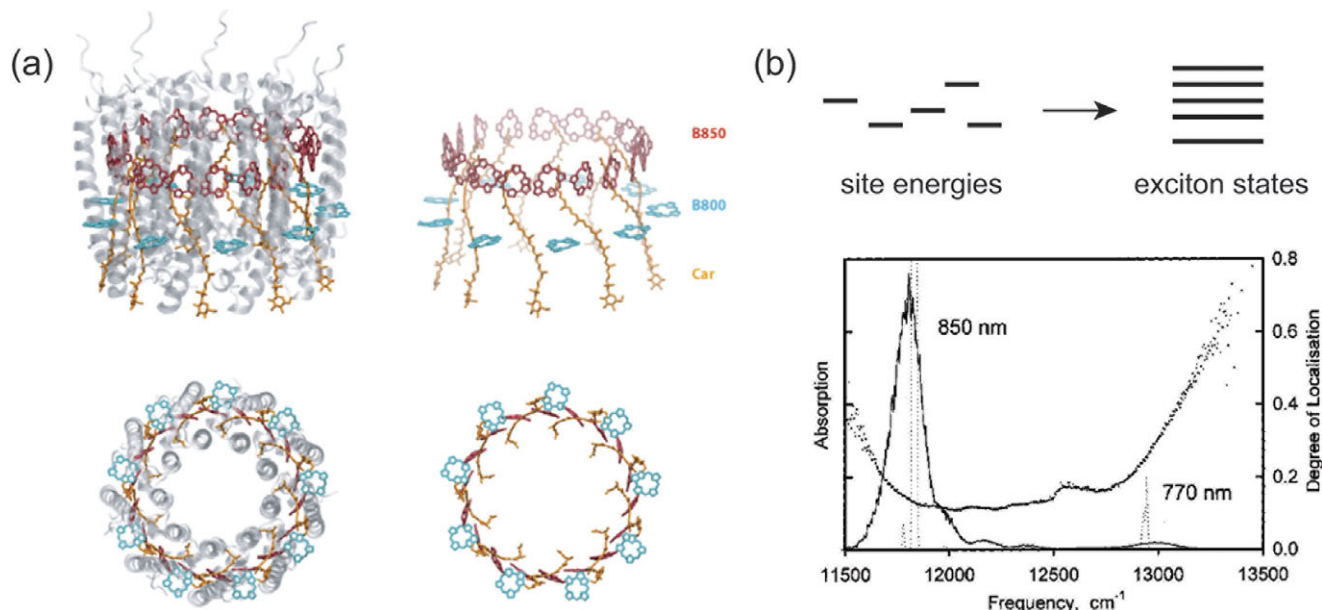
Figure 2. (a) Structural model of LH2 showing the two rings of BChl chromophores, B800 (blue) and B850 (red). (b) Disorder in the site energies of chromophores in the B850 band change the exciton density of states, causing the excitons to be less delocalized. Adapted with permission from (Scholes *et al.* 1999) copyright 1999 American Chemical Society.

yield ϕ_D and fluorescence lifetime τ_D, solvent refractive index n, and the overlap integral between the fluorescence spectrum of the donor and the absorption spectrum of the acceptor,

$$k_{Forster} = \frac{constants}{n^4} \times \frac{\phi_D}{\tau_D}\frac{\kappa^2}{R^6}\int_0^\infty dv\alpha_A(v)f_D(v). \quad (1)$$

Here, the donor fluorescence spectrum $f_D(v)$ is area normalized on a frequency scale and the acceptor absorption spectrum $\alpha_A(v)$ is plotted quantitatively as molar extinction. The equation contains the donor–acceptor center-to-center separation R and an orientation factor for the dipole–dipole coupling between donor and acceptor transition dipoles,

$$\kappa = \widehat{\mu}_D.\widehat{\mu}_A - 3\left(\widehat{\mu}_D.\widehat{R}\right)\left(\widehat{\mu}_A.\widehat{R}\right),$$

where the 'hat' means unit vector.

If we collect the dipole strength terms from ϕ_D/τ_D and $\alpha_D(v)$, changing the latter quantity to the area normalized absorption spectrum $a_A(v)$, then Eq. (1) becomes

$$k_{Forster} = \frac{constants}{n^4} \times \left(\frac{\kappa\mu_D\mu_A}{R^6}\right)^2\int_0^\infty dv\alpha_A(v)f_D(v). \quad (2)$$

Where now it is clear that the EET rate is in the form of the Fermi Golden Rule; it is written as a product of the weak electronic coupling (the perturbation that couples the donor and acceptor) and a spectral overlap that ensures energy conservation and accounts for the temperature dependence of energy transfer. The spectral overlap accounts for the density of isoenergetic states.

We will use this equation as a reference for explaining how energy transfer happens in the intermediate coupling regime relevant to photosynthetic light harvesting. By keeping in mind, the intuitive spectral basis for Förster theory – the fluorescence spectrum of the donor overlaps the absorption spectrum of the acceptor – we will discuss how and why new experiments in new theoretical descriptions were needed to explain the mechanism of photosynthetic light harvesting.

Excitonic structure of light-harvesting complexes

Soon after the structure of LHC LH2 from purple photosynthetic bacteria was solved, we knew the key ingredients deciding the biophysics of EET in LH2, and likely other LHCs. These were electronic couplings, disorder in the site energies (i.e., absorption peaks of the chromophores) which comes about because of local structure variations in the proteins, and the intrinsic homogeneous line broadening of the spectra.

The approximations underlying Förster theory mean that, for a donor–acceptor system, details of the spectral line broadening do not matter – we only need the band shapes. An accurate theory, however, requires more detail (as we describe below). The LH2 structure (Cogdell *et al.*, 2006) shows how the BChl *a* molecules in the 'B850 ring' (Figure 2a), are closely spaced, and therefore interact strongly. That strong electronic coupling suggests that the absorbing states could be coherently delocalized around the entire ring – molecular exciton states. However, the disorder in the site energies has a localizing effect (Figure 2b), and this interesting problem was the first to be attacked by simulations.

The question about localization versus delocalization of the B850 excitons is interesting because the electronic couplings between adjacent BChl *a* molecules are similar in magnitude to the standard deviation of the site energy disorder. This prominence of disorder in the site energies was known from hole burning experiments (Wu *et al.*, 1997) and from the temperature dependence of the fluorescence spectrum. Various simulations like those shown in Figure 2b concluded that exciton states in B850 are likely delocalized over about four molecules, not all 18. What is shown in Figure 2b is a calculation of the B850 absorption spectrum in the limit of inhomogenous line broadening. Random energy offsets are added to the site energies before the Hamiltonian matrix of each replicate of the complex is diagonalized,
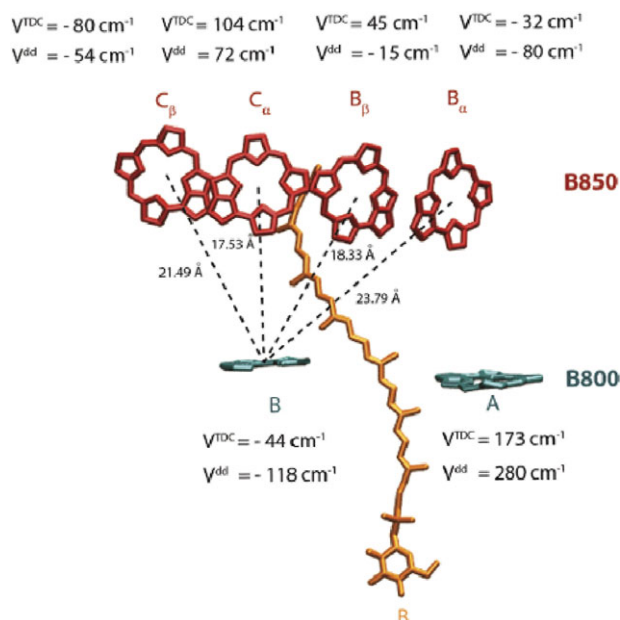
Figure 3. Calculations of electronic (Coulombic) couplings between BChl a molecules in LH2 using the TDC method (V^{TDC}) compared to estimations based on the dipole approximation (V^{dd}). Adapted from (Krueger *et al.* 1998), copyright 1998 American Chemical Society.

then the results are ensemble averaged – giving the spectrum as a histogram. We can also calculate the 'inverse participation ratio', which gives an estimate for the number of BChl molecules, on average, over which the excitation is delocalized (Fidder *et al.*, 1991; Scholes, 2020).

The delicate interplay between disorder and electronic couplings means that accurate estimation of electronic couplings is an important basis for accurate predictions of excitonic states and energy transfer dynamics. Electronic couplings are the backbone for modeling spectroscopic data and energy transfer dynamics. They provide the link between models and structure. The starting point was to elucidate an accurate theoretical description of the relevant electronic couplings for energy transfer and develop new ways to calculate them. At the time, contemporary thinking was strongly influenced by the dipole–dipole model intrinsic to Förster theory and Dexter's theory for coupling between closely spaced atoms that considered the exchange interaction contributed by orbital overlap and higher multipole coupling terms.

The first issue to clear up was that dipole–dipole coupling (or, more generally, Coulombic coupling between transitions) and orbital-overlap mediated coupling are not mutually exclusive (Scholes *et al.*, 1999). That is, EET does not happen by a Förster mechanism *or* a Dexter mechanism – instead, for closely interacting chromophores, both classes of coupling mechanism may operate together. As an illustration, see Figure 7 in Mirkovic *et al.* (2017). It was difficult to calculate the orbital-overlap mediated coupling, especially because it was not widely realized that the exchange contribution was a minor contributor for interacting molecules (Scholes *et al.*, 1995). The orbital-overlap mediated coupling can be significant at inter-chromophore spacings of approximately 4 Å or less, and it grows exponentially as distance diminishes. Since the inter-BChl *a* spacing in the B850 ring approaches this length scale, this contribution to the coupling needed to be assessed. Quantum chemical calculations (Scholes *et al.*, 1999) indicated that the orbital-overlap mediated coupling between nearest-neighbor BChl *a* chromophores in B850 are about 25% as large as the Coulombic interaction.

The challenge, with wider implications across all LHCs, was to go beyond the dipole–dipole coupling approximation. It turns out that when the molecular donor–acceptor separation is comparable to the size of the molecular chromophores, the multipole expansion does not converge, and is therefore unhelpful as a way of improving the estimate of electronic coupling. The multipole expansion works well only when the dipole approximation is already a good approximation, which was found not be the case for electronic couplings in LHCs.

The problem needed to be considered anew. We knew a lot about calculating the interaction between static charge distributions of arbitrary shape and size, and it was evident that one did not have to make a multipole expansion to approximate these charge distributions. It would make sense simply to coarse-grain the charge into cells and sum all the Coulombic interactions between cells. The step needed to apply this idea for the electronic couplings in EET was to realize that the relevant charge distributions are quantum mechanical entities known as transition densities. Further, it was possible to calculate transition densities with quantum chemical methods and save them as discretized charge densities, which we called TDCs. On this basis, electronic couplings could be easily calculated accurately without needing to make a multipole expansion (Krueger *et al.*, 1998).

We applied the TDC method to calculate electronic couplings in LH2 (Figure 3). Those calculations highlight the problem with the dipole approximation when large chromophores are positioned close together – its success is poor, or at best unpredictable. We can see from some of the results shown in Figure 3 that sometimes the dipole approximation works, sometimes it predicts a significantly wrong magnitude, and sometimes it predicts the wrong sign for the coupling.

It struck us at the time that it is curious that the dipole approximation works so reliably for electronic spectroscopy, yet it fails for interchromophore couplings in LHCs. The physical insight is that light, having a wavelength much larger than the size of the molecule, averages 'in the far field' over the details of molecular shape, and hence the transition density. In contrast, a nearby acceptor molecule sees the donor in the 'near field', and hence resolves the shape of the transition density. Moreover, the way the molecules 'see' each other is to trace out the Coulomb interaction, which goes as $1/r$ and therefore strongly biases coupling to the closest regions of the transition densities, breaking the symmetry of the far-field view. Hence, the shapes of the donor and acceptor molecules have a significant impact on the Coulomb interactions, which is evident in Figure 3 by the carotenoid–BChl *a* interactions compared to those estimated by the dipole–dipole coupling.

Further significant advances include the development of the TrEsp (transition charge from electrostatic potential) method by Madjet *et al.* (2006), which provided significant gains in computational efficiency while predicting electronic couplings accurately – even accounting for environmental effects (Renger and Müh, 2012). Mennucci and Curutchet made significant advances in understanding how polarizable environments, such as solvent, 'screen' electronic couplings (Curutchet and Mennucci, 2005; Curutchet *et al.*, 2007; Scholes *et al.*, 2007). Other developments (Curutchet and Mennucci, 2017) include inclusion of the effects of the protein environment on coupling calculations (Curutchet *et al.*, 2011).

At this point, it made sense to think about more elaborate theories for EET dynamics. A starting point was to address the fact that the static model, where excitonic structure is determined solely by the interplay of electronic coupling and disorder, does not give the entire picture. Different kinds of experiments concluded different delocalization lengths, reflecting the notion that excitons

start out more delocalized than they are at equilibrium. For example, analysis of circular dichroism data (Koolhaas *et al.*, 1998) suggested that excitons are delocalized throughout the ring upon absorption of light, whereas superradiance indicated a delocalization length of 2–4 molecules (Monshouwer *et al.*, 1997). Pullerits *et al.* (1996) used pump–probe spectroscopy to estimate delocalization as a function of time by comparing the intensities of the excited state absorption (ESA) and bleach bands. They found evidence for a more delocalized initial state that localized somewhat with time, and concluded the need for a 'unified approach' to calculate exciton dynamics, that is, a more sophisticated theory was needed. The idea of dynamic localization was supported by other studies. Therefore, the EET theory needs to account for self-consistent dynamic interactions between the molecular excitons and the environment fluctuations.

As a starting point, we needed to work out how delocalized exciton states operate in light harvesting (Jang and Mennucci, 2018). Do they provide a way to speed up EET? As discussed above, in an effort to close the gap between Förster theory prediction and experimental observations (Jordanides *et al.*, 2001; Scholes *et al.*, 2001), we realized how this 'near field'/'far field' insight was also needed to understand how delocalized molecular exciton states act as donors and/or acceptors in EET. Modifying Förster theory to accommodate the model led to GFT (Scholes and Fleming, 2000) as described earlier. A key finding of that work was that dark exciton states can be excellent donors or acceptors, even though Förster theory predicts that dark states cannot transfer nor accept excitation, because they have zero dipole strength. GFT explained the long open question of the EET rate measured for the RC of purple bacteria and it quantitatively resolved the B800 to B850 EET rate in LH2. The method was later elaborated further, especially by Jang (2011), Jang and Cheng (2013), and Jang *et al.* (2004).

A physical insight gained from GFT calculations was that the B850 absorption spectrum needs to be deconvolved into a set of acceptor densities of states, one for each exciton state. The EET rate is calculated by ensuring that each of these acceptor density of states is associated with its unique electronic coupling term that we labeled coupling-weighted spectral overlaps. Keeping account of this averaging procedure is especially important in view of the B850 site energy disorder. The bigger picture is that how one performs averages for the ensemble matters – we cannot simply average the spectral overlaps and average the electronic couplings then multiply, for example. Hence, even in relatively simple models, there are correlations that must be accounted for. That theme will be continued in the next section.

The challenge in understanding the ultrafast dynamics was how to capture the way states, dynamics of EET, and spectroscopic signatures evolve in time as a balance is attained between electronic couplings that delocalize states and the localizing effects of site energy disorder and energy fluctuations that enable excitations to migrate among the chromophores in LHCs (Ishizaki and Fleming, 2009a,b; Renger, 2009; Novoderezhkin and van Grondelle, 2010). The dynamical properties of energy gap fluctuations that underpin homogeneous line broadening in spectroscopy (Fleming *et al.*, 1998) present a particular challenge. Interestingly, it was known that the Stokes shift of Chl *a* (and likely BChl *a*) in LHCs is surprisingly small (Szalay *et al.*, 1974) – meaning so is the amplitude of spectral energy gap fluctuations – so the system-bath coupling is smaller than one would expect. This is somehow enabled by the protein environment. The observation hints at a design element relevant to efficient light harvesting. Indeed, Jimenez *et al.* (1997) wrote that this weak system-bath coupling 'is likely to be one of the most important factors underlying the efficiency of the energy

---

Box 1. Open questions in 1997.

Can electronic couplings be calculated accurately enough using the dipole approximation? If not, how do we calculate them?
How does excitation energy move on timescales comparable to, and interplaying with, energy gap correlations in spectral lineshapes, the dynamic Stokes shift, and changing delocalization of exciton states?
How does the disordered energy landscape throughout light-harvesting complexes help efficient and robust long-range energy transfer?
Is the energy transfer best described as coherent or incoherent?

---

transfer processes in LH1 and LH2 complexes'. However, it took new experimental developments over the following decade to shed light on how to understand why this is the case. In Box 1, we list some open questions in the field at this point, around 1997.

While we illustrate our main points in this article using just a few examples of LHCs, it is worth noting the incredible diversity of LHC structures (Scholes *et al.*, 2012) (Figure 4). They range from proteins with a diameter of about 5 nm, binding eight chromophores, to massive aggregates comprising around 200,000 BChls inside a lipid–protein 'shell'. Thus, there exists several complementary 'test-beds' for experiment and theory to collaborate in the elucidation of models and design principles for light harvesting.

The development of two-dimensional electronic spectroscopy

It turns out that the quest to answer the questions posed above motivated the need for new spectroscopies where we can go beyond measurements of kinetics and start to probe spectral correlations and their interplay with excited state dynamics. We will return to discuss this 'need' in the following section, but first, we introduce two-dimensional electronic spectroscopy (2DES).

As various new ultrafast laser experiments were invented and applied, it became difficult to understand how to compare data from one experiment to another. It was also difficult sometimes to appreciate deeply what was being measured. We needed a common framework for categorizing, understanding, and designing nonlinear spectroscopies. Addressing this need, Mukamel (1995) developed a highly intuitive set of tools that has enabled experimentalists to understand electronic and vibrational dynamics in complex molecular systems. His unified superoperator density-matrix framework and 'Liouville space pathways' created the standard language for the design and interpretation of coherent ultrafast nonlinear optical experiments in terms of the now ubiquitous double-sided Feynman diagrams. In that way it crystallized advances in understanding how to devise and interpret cutting edge experiments.

The development of a systematic formalism enabled photon echo spectroscopies to be developed to study transition energy gap fluctuations and EET in LHCs. These methods turned out to be very good for characterization of lineshape correlation functions for solvated chromophores and for quantifying inhomogeneous line broadening (Cho and Fleming, 1996; Fleming *et al.*, 1998), and that information has close connections with theoretical methods (Tanimura, 2006). The information learned from various nonlinear spectroscopies, like photon echo experiments, made it evident that ultrafast EET in LHCs happens on timescales not too different than lineshape correlation times. Moreover, the experimental results emphasized the importance of developing photon echo-type experiments further. But how?

In a 1993 article, Tanimura and Mukamel (1993) had proposed a new class of coherent measurements that use sequences of multiple femtosecond pulses in order to gain structural and dynamical information unavailable from linear techniques. Extending ideas
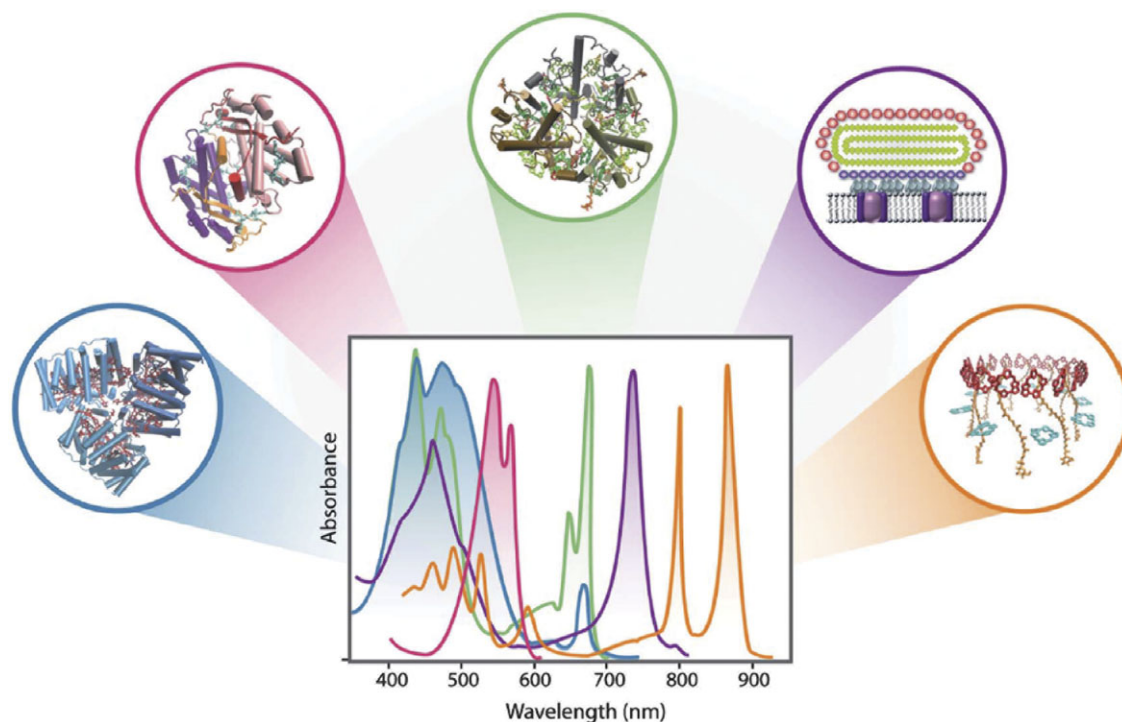
Figure 4. Light harvesting complexes. Variation in light-harvesting antennae commonly encountered in photosynthetic organisms, which vary widely in their protein structure and the number and arrangement of pigments utilized. The molecular structures (with parent organisms in brackets) from left to right are: peridinin chlorophyll protein or PCP (of *Amphidinium carterae*), phycoerythrin 545 (of *Rhodomonas* CS24), light harvesting complex LHCII (of *Spinacia olearia*), schematic representation of a chlorosome (of *Chloroflexus aurantiacus*), and light harvesting complex LH2 (of *Rhodopseudomonas acidophila*). Their respective absorption spectra, shown in matching colours, illustrate how different organisms have evolved to optimize their light-harvesting capabilities in different regions of the visible spectrum. Figure adapted with permission from (Scholes *et al.* 2012), copyright 2012 Royal Society of Chemistry.

from Nuclear Magnetic Resonance (NMR) to the optical regime, they showed how analogous, but different information can be extracted by combining heterodyne detected phase-controlled weak field signals generated at different phase matching directions.

This work pointed to the next goal. Researchers needed to develop strategies for the design of pulse sequences in coherent vibrational and electronic spectroscopies that accomplish the same goals as multidimensional liquid or solid-state NMR by control over coherence transfer pathways. An obvious challenge was that the spectroscopic analogs would be much more difficult to implement in experiment because they involve several orders of magnitude faster timescales than NMR methods. For example, one technical difficulty for putting the 2DES experiment into practice is to shift from scanning time delays between pulse envelopes to requiring pulses to sweep stably across each other's electric field under the pulse envelope. Therefore, the experiment requires not only generation of phase-locked pulse pairs, but also a way to delay the timing in the pump pulse pair with sub-attosecond precision (Turner *et al.*, 2011).

The next step for learning about mechanisms of light harvesting was to develop and apply multidimensional nonlinear spectroscopies (Gallagher *et al.*, 1998; Hamm *et al.*, 1998; Jonas, 2003a; Brixner *et al.*, 2004; Hochstrasser, 2007). Multidimensional techniques provide a wealth of information: new peaks, their intensities, and profiles give a direct signature of molecular structure (distances between chromophores) and dynamics (the spectral density of the chromophores' environment). Two-dimensional correlation plots show distinct signatures of energy level fluctuations and their characteristic timescales and degree of correlation by variations of the cross-peak lineshapes.

There are several reviews available that give detailed technical introductions and viewpoints on 2DES (Jonas, 2003b; Cho *et al.*, 2005; Cho, 2008; Ogilvie and Kubarych, 2009; Schlau-Cohen *et al.*, 2012; Biswas *et al.*, 2022; Fresch *et al.*, 2023). Key papers reviewing relevant theory include Abramavicius and Mukamel (2004), Abramavicius *et al.* (2009), Mukamel (2000), and Zhang *et al.* (1998). Briefly, 2DES enables two main advances over prior methods. First, it yields a time sequence of spectroscopic maps that indicate how population of the excited states flows among the states. Second, because these maps are closely tied with the density matrix of the evolving ensemble of states, 2DES can more incisively detect and allow assignment of coherent wavepackets, generated by femtosecond pulses, and their subsequent evolution in time. A list of advantages offered by 2DES is given in Box 2.

A quick description of how the experiment is carried out is given here, and see Figure 5. The cleanest explanation is to assume that we use two pump pulses, a probe pulse, and a local oscillator impinging in the sample with different incident vectors, usually the BOXCARS geometry. The signal is produced 'background free' in the same direction as the local oscillator. Thus, we describe the signal generation only for the processes that lead to this phase-matched signal field. The excitation in 2DES is performed by a phase-locked pulse pair. The idea is to vary a time delay between these pulses (the 'coherence time', τ) so that the population grating written in the sample by interaction of the sample with the interference pattern of the pulse pair is encoded within the excitation frequency axis, exposed after Fourier transformation with respect to this 'coherence time' delay. The probe pulse is scanned as a function of the 'population time', T (also known as 'waiting time'), which is equivalent to the usual concept of a pump–probe time delay. The probe picks up the pump sequence frequency encoding as it stimulates a radiated signal field that, effectively, diffracts off the population grating. The signal is measured using a spectrometer to resolve the signal frequency axis of the 2D map.
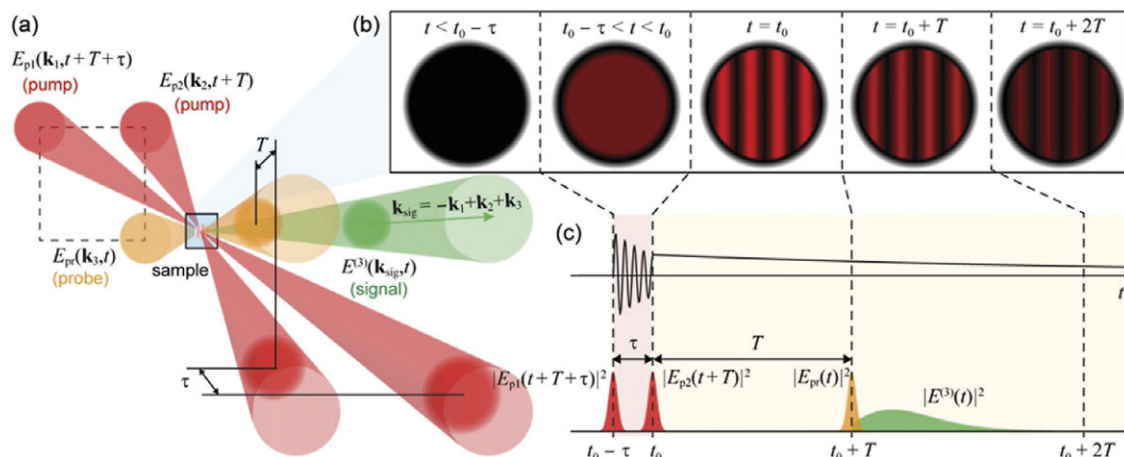
Figure 5. (a) Schematic representation of a 2DES experimental setup. (b) Spatial distribution of molecules of interest in the ground (back) and an excited (red) states, where t_0 is the moment that the second pump (p2) pulse reaches the sample. (c) The nonlinear response of the sample (top) and the four interacting pulses (bottom). Reprinted with permission from (S Biswas *et al*. 2022), copyright 2022 American Chemical Society.

Box 2. Features of two-dimensional electronic spectra.

- Greatly improved spectral resolution in congested spectra because the spectrum is resolved in two dimensions.
- Diagonal and cross peaks are resolved and each provide complementary information.
- Antidiagonal cuts of rephasing spectra can eliminate or greatly reduce inhomogeneous broadening.
- Cross peaks reveal couplings between components of complex systems.
- The time-dependent evolution of cross peaks reveals pathways of relaxation in multicomponent systems.
- Coherent 2D spectra are especially sensitive to oscillations in amplitude from coherences (superpositions) between electronic, vibronic (mixed electronic and vibrational), and vibrational states, mainly because of the way features are spread out in the spectra.
- Frequency beating maps recorded in rephasing and non-rephasing pulse sequences can be used to distinguish electronic and vibronic coherences from vibrational coherences (vibrational wavepackets).
- The evolution of the shape of the diagonal peaks provides information about the timescale and mechanism of the interaction of the system and the environment.

We note that there are three types of 2D spectra can be recorded according to the way the pulses are scanned relative to each other: (1) rephasing spectra where the photon echo pulse sequence is used, corresponding to the phase-matching condition $-k_1 + k_2 + k_3$, (2) non-rephasing spectra where the free induction decay pulse sequence is used, corresponding to the phase-matching condition $k_1 - k_2 + k_3$, and (3) absorptive 2D spectra, which are the sum of (1) and (2). The examples shown in the following section give a little insight into how these different 2DES spectra have been exploited to learn about photosynthetic light harvesting. In Figure 6, we give a schematic overview of the different kinds of 2DES spectra we will discuss.

There have also been advances enabled by using polarization sequences in 2DES spectroscopy. Polarization control of the pulses was initially challenging because it made it difficult to set the overall phase of the electric fields, but that difficulty was overcome by later developments in producing and employing phase-locked pulses. Polarization control has enabled discrimination of different cross-peaks and enhanced characterization of 2D spectra (Read *et al*., 2007; Milota *et al*., 2009; Westenhoff *et al*., 2012; Thyrhaug *et al*., 2016; Thyrhaug *et al*., 2018; Palecek *et al*., 2019).

The need for more incisive experiments

To motivate why new experiments were needed, here we discuss briefly how the EET theory changes when we cannot assume that electronic coupling is much smaller than the bath reorganization energy (half the Stokes shift). While fundamental theories for activated rate processes and developments during the 1980s, in particular, set the scene for how dynamics happen in the condensed phase (Frauenfelder and Wolynes, 1985; Wolynes, 1987), EET should be thought about differently. For example, energy migration among alike molecules, such as Chl-to-Chl EET, appears to be essentially an activated process because the Stokes shift between absorption and fluorescence indicates that the donor needs to go 'uphill' in energy to attain resonance with the acceptor absorption. However, we cannot understand EET in terms of a single energy landscape – fundamentally it involves the coupling of two electronic transitions, meaning we need to keep four states in mind (in the local molecular basis).

An important microscopic ingredient in EET theory is how the solvent and other environmental degrees of freedom introduce energy gap fluctuations in the two coupled transitions. Those fluctuations introduce energy offsets and energy resonances between donor emission and acceptor absorption. Energy resonances in the presence of electronic coupling allow excitation to delocalize, whereas energy offsets give disorder, which has a localizing effect. Moderate to strong electronic coupling modifies this trajectory of stochastic energy gap fluctuations as a function of time by requiring the transient donor–acceptor energy differences to be larger in order to uncouple resonances – exciton delocalization becomes more persistent or robust.

Now, the key point for developing realistic theories for the dynamics, and hence for ascertaining what we really need to measure in experiments, is that the energy gap fluctuations are correlated with some characteristic time scale – making the dynamics 'non-Markovian'. In activated rate theories, we often think of this physically as a kind of friction. In the case of EET, we can think of electronic coupling introducing an additional correlation between the spectral fluctuations of the donor fluorescence and the acceptor absorption because it mixes those states slightly – delocalization switches on and off transiently for time windows dictated by correlations in the fluctuations. This more elaborate physical picture, although here explained qualitatively, indicates why the electronic coupling and spectral overlap are generally not
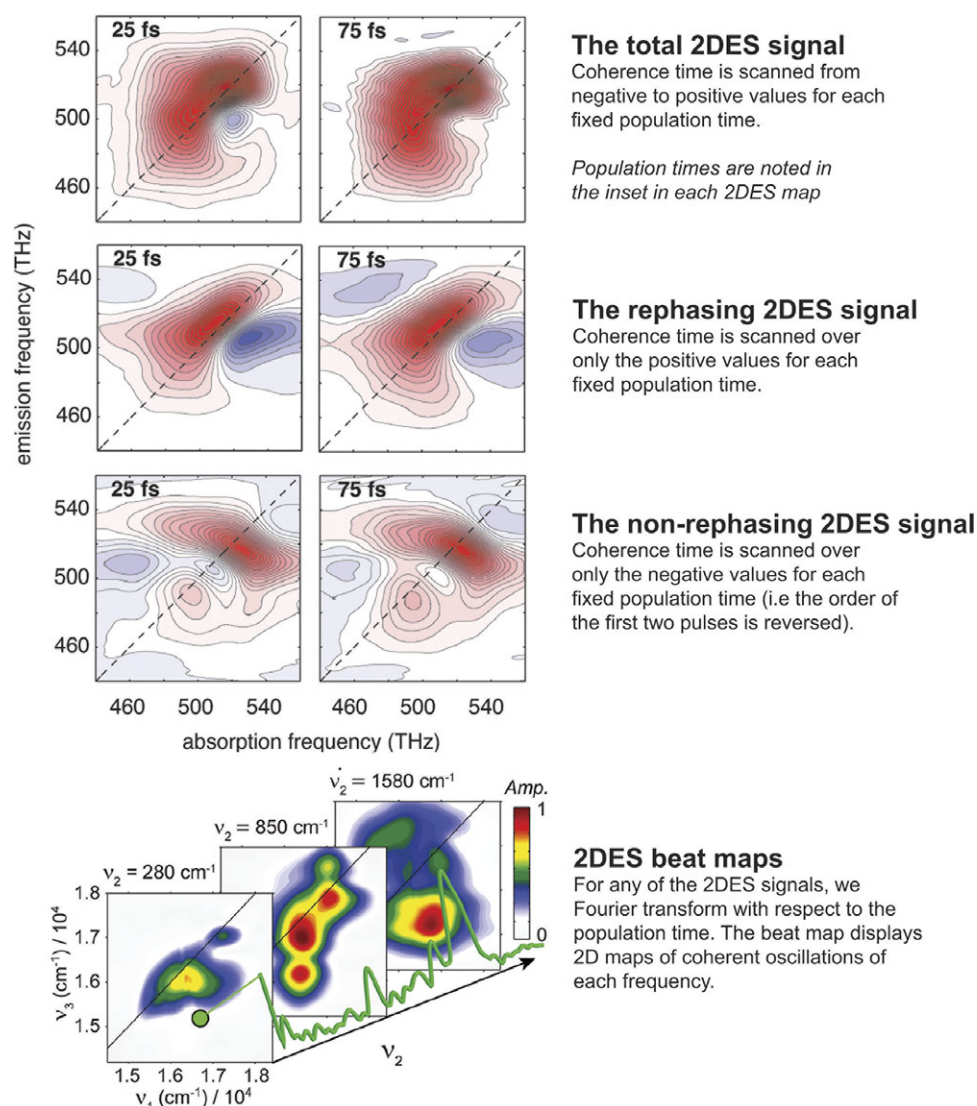
Figure 6. Overview of the various 2DES experiments and data representations. The data are for the PC645 light-harvesting complex. Adapted from (Dean and Scholes 2017; Turner *et al.* 2012), copyright 2017 American Chemical Society and copyright 2012 Royal Society of Chemistry (Great Britain), respectively.

separable, in contrast to the assumptions inherent in Förster theory.
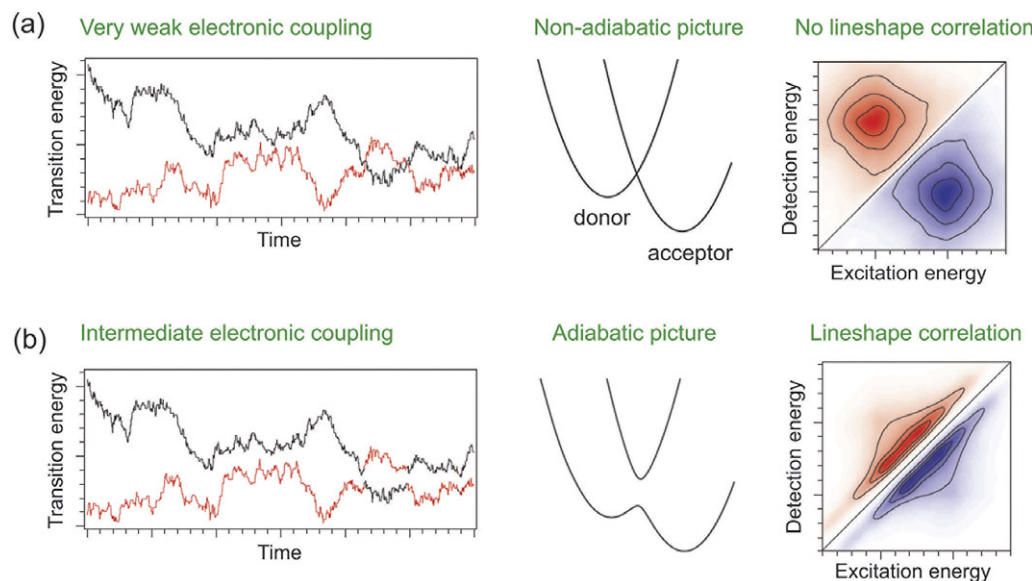
Detecting the tell-tale spectral correlations between donor and acceptor with an experiment would clearly distinguish the intermediate EET mechanism from incoherent hopping predicted by Förster theory because the spectral fluctuations are assumed in Förster theory to be entirely uncorrelated. What was clearly demanded was to make a step change away from measuring rate *constants*, and instead probe signatures of mechanism. For example, an experiment that measures correlations between donor fluorescence and acceptor absorption during the EET would provide crucial insights. This need is enabled by 2DES.

A simple pedagogical example might provide intuition for how 2DES can be exploited to learn about EET dynamics beyond the Förster model. Figure 7a shows a simplified model for visualizing transition energy fluctuations as a function of time for two independent, very weakly coupled and uncorrelated molecules (Wong *et al.*, 2012). The distribution of transition energies gives the free energy curves shown. The electronic coupling is very weak, so it acts as a perturbation for activated hopping from the free energy curve of the donor to the acceptor. This is usually called the nonadiabatic

picture for dynamics or, equivalently, the diabatic picture. This is a Förster model. In the energy trajectory picture, the excitation can hop from donor to acceptor any time the fluctuations bring the transition energies close to resonance – in the ensemble average, this translates to the Förster spectral overlap. Corresponding 2DES spectra would show no correlations between the donor and acceptor spectra in the off-diagonal line shapes.

In Figure 7b, we modify the example described above by adding a larger electronic coupling between the donor and acceptor. Notice that now the trajectories never cross because the electronic coupling 'repels' them by forming coherent superposition states (exciton states) when the trajectories come close in energy (comparable to the electronic coupling). We see that mixing in the ensemble picture has avoided crossing of the free energy curves, introducing adiabatic dynamics in the curve crossing region. The fluctuating delocalization in the energy gap trajectories introduces a correlation between the donor and acceptor spectra, revealed by elongation of the corresponding 2DES cross-peaks.

How does gathering a deeper understanding of EET in the intermediate coupling regime matter? One obvious outcome has been that this challenge has stimulated the development of new

Figure 7. The principle of 2D correlation spectroscopy for detecting donor-acceptor spectral correlations. (a) Segments of excitation energy trajectories for two independent chromophores, the corresponding ensemble free energy curves, and simulated 2DES correlation in the rephasing cross-peak spectrum. (b) Similar to (a) except that the two chromophores are electronically coupled. The red line indicates that the eigenstate has more amplitude of excitation on the donor chromophore than on the acceptor, and vice versa for the black line. Reprinted from (Wong *et al.* 2012), copyright 2012 Springer Nature Limited.

theoretical tools and experiments that push the forefront of the field. A key practical realization has been that this difficult, intermediate coupling regime happens to be where EET is most efficient – a principle denoted the Goldilocks principle for energy transfer (Rebentrost *et al.*, 2009b). It turns out that a little coherence, but not too much, can help move excitation energy faster than either in the Förster limit of localized hopping, or in the limit where all excitons are delocalized (Ishizaki and Fleming, 2012; Chenu and Scholes, 2015).

As a starting point, we describe in the next section, some examples of how 2DES provides maps of spectroscopic states, and how we interpret those dynamical maps. After that, we return to the central ideas of this section – how can 2DES elucidate more specific details about light-harvesting mechanisms?

Two-dimensional spectroscopy maps pathways of light harvesting

The application of 2DES to study LHCs provided a sequence of influential insights. The first work, reported by Brixner *et al.* (2005), was to map energy flow by EET within the Fenna–Matthews–Olson (FMO) complex isolated from photosynthetic green sulfur bacteria (Figure 8). The 2DES spectrum lays out the ground state absorption spectrum along the diagonal part of a map that correlates excitation frequencies to detection frequencies. As energy flows from one spectral band to another, a corresponding cross-peak grows in with time that quantifies population kinetics for interconversion of the species associated with those bands. The cascade of cross-peak growth can be analyzed fairly simply to elucidate a map of kinetics. Those kinetics can be, in turn, mapped onto the structural model for the complex because site energies – that is, the spectral bands for various BChl *a* species in the complex – can be ascertained using spectroscopy combined with techniques such as site-directed mutagenesis.

Thus we obtain a remarkably detailed picture of the femtosecond and picosecond kinetics of EET after photoexcitation (Figure 8a,b). The data reported by Brixner *et al.* are shown in Figure 8c. More

recent data from the Engel group (Hayes and Engel, 2012) are shown in Figure 8d. Two main photoexcitation transfer pathways were found by the experiments, shown by red and green arrows in Figure 8b. A key conclusion is that energy transport is not just a simple stepwise process where energy flows 'downhill', that is, from one level to the next level below. Instead, the EET dynamics are dictated by a combination of spectral overlap and spatial proximity, hinting that electronic coupling cannot be considered 'weak'.

To understand the value of 2DES, it will be useful first to recall the typical approach for obtaining this information using femtosecond pump–probe techniques. It is obtained by analyzing the transient probe spectrum, which is equivalent to the projection of the 2DES spectra onto the detection axis. In pump–probe spectroscopy, then, resolution of excitation frequency is lost with the result that many peaks that are clearly separated in 2D spectra overlap in transient pump–probe spectra. The information content in the 2DES spectrum is much more clearly presented, thus, in principle, allowing more complicated kinetic schemes to be uncovered.

Some other 2DES experiments provide examples that we present qualitatively to illustrate how the peak-resolving power of the experiment can be exploited to identify the spectral location of exciton peaks.

The vast majority of Chl on Earth is bound in a LHC called LHCII. The LHCII protein is a trimer that binds, in total, 42 Chls (both Chl *a* and Chl *b*; Figure 9a). Owing to the large number of Chls bound in LHCII, even at 77 K, the absorption spectrum is highly congested. While it is clear that the spectrum is broadened by various kinds of heterogeneity, including the different chromophores (Chl *a* and Chl *b*), site energy disorder, and exciton splitting, it is difficult to deconvolve those features by assigning spectral features such as indicated by the sticks in Figure 9b. Collectively, these features spread across the spectrum decide the energy landscape within the protein, which plays a key role in controlling the mechanism of light harvesting – thus it is important to resolve.

A key step toward measuring the energy landscape of LHCII was made by (Calhoun *et al.*, 2009). They showed how to analyze oscillating features in the 2DES spectra (Figure 9c), in order to
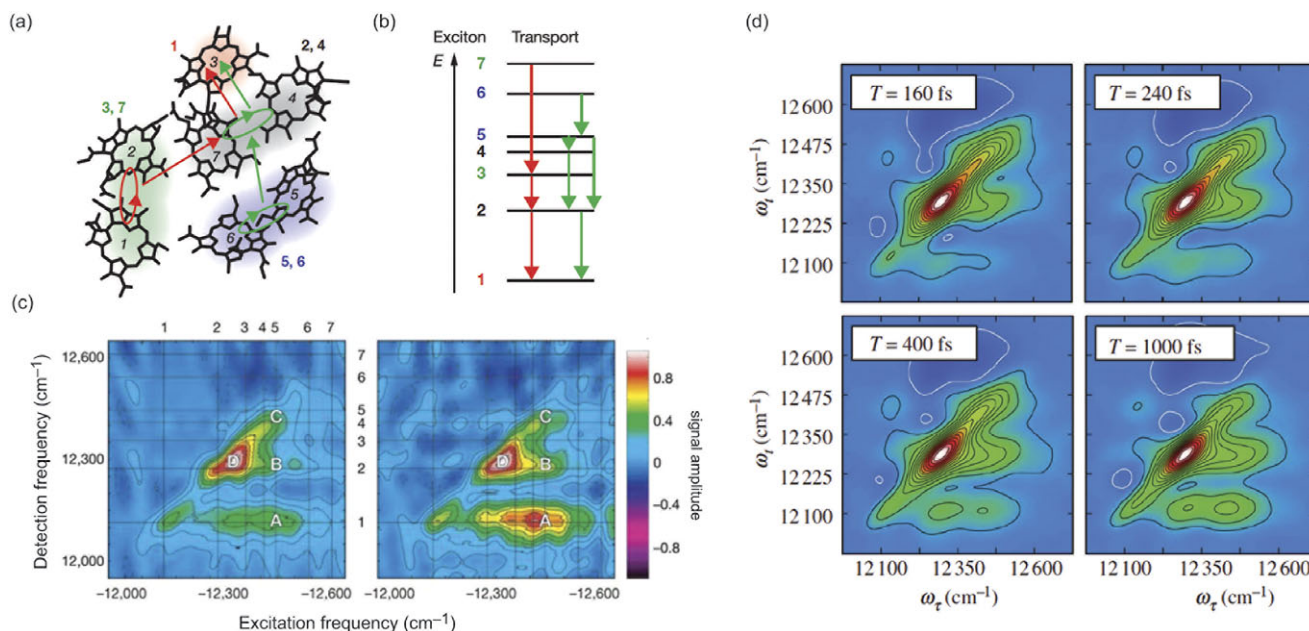
Figure 8. (a) The structural arrangement of the seven BChl molecules in the FMO structure is overlaid with shadings that indicate the delocalization patterns of the different excitons. (b) Two main photoexcitation transfer pathways were indicated by the experiments, shown by red and green arrows. (c) Experimental 2DES spectra (Brixner *et al.* 2005) (real parts) of the FMO complex from *Chlorobium tepidum* at 77 K. Reprinted from (Brixner *et al.* 2005) with permission, copyright 2005: Macmillan Magazines Ltd. (d) A series of two-dimensional spectra of FMO taken at increasing values of population time, *T*. The spectra show the real (absorptive) part of the signal from both rephasing and non-rephasing response pathways. The color and contours lines are scaled linearly. Black contour lines correspond to positive features and white contour lines to negative features. Reprinted from (Hayes and Engel 2012), copyright 2012 The Royal Society.

assign the exciton bands. It is remarkable, given the spectral complexity of LHCII, how well those coherences can be resolved. The technique succeeds because even if excitons share a similar spectral position, they can usually be distinguished by different patterns in cross-sections through the 2DES 'beat map' (refer to Figure 6). It turns out that a similar strategy can be pursued, much more spectacularly, using 2DEV spectroscopy, as we describe later.

In a related paper, Schlau-Cohen *et al.* (2009) used 2DES to study the flow of excitation energy in LHCII. Analysis of the 2DES data included spectra known as 'non-rephasing' spectra that are obtained by a particular scan sequence when collecting the data (Figure 10*a*). The analysis resolved two distinct pathways for the energy flow (Figure 10*b*). One pathway transfers excitation from the luminal side of the membrane-bound LHC to the stromal side, a vertical path. The other pathway relocates energy around the stromal part of the complex. An important insight from this work was not only the resolution of these pathways, but the assignment of small groups of Chls that are strongly coupled, thus forming excitonic states that help direct the flow of excitation. These clusters of coupled chromophores are shown in Figure 10*c* by the yellow circles. The major pigments with contributions to each exciton were determined by fitting all the data to a Hamiltonian-based model. The excitonic energies were found with the aid of the electronic coherence beating signal.

In this review, we explicitly discuss only a few selected examples, but of course, there are many other examples of the application of 2DES to study photosynthetic systems. A narrow selection illustrates the breadth of topics and questions that have been studied, including carotenoids in various LHCs (Ostroumov *et al.*, 2013; Roscioli *et al.*, 2017, 2018; Toa *et al.*, 2019; Son *et al.*, 2020a, 2021; Tilluck *et al.*, 2021; Tumbarello *et al.*, 2022), charge separation in photosystems and dynamics of complexes containing RCs (Myers *et al.*, 2010; Lewis and Ogilvie, 2012; Westenhoff *et al.*, 2012; Fuller *et al.*, 2014; Romero *et al.*, 2014; Dostál *et al.*, 2016; Ma *et al.*, 2017,

2018, 2019; Lee *et al.*, 2018; Niedringhaus *et al.*, 2018; Song *et al.*, 2019, 2021b; Policht *et al.*, 2022; Nguyen *et al.*, 2023b), and LH2 (Zigmantas *et al.*, 2006; Dahlberg *et al.*, 2013; Fidler *et al.*, 2013, 2014; Perlík *et al.*, 2015; Schröter *et al.*, 2018; Massey *et al.*, 2019; Sardjan *et al.*, 2020; Kim *et al.*, 2021, 2022a; Thyrhaug *et al.*, 2021).

## Coherent oscillations and mechanistic insights from 2DES

Yet, 2DES spectroscopy contained much more information than solely kinetics, and this is where the potential for new physical insight is most significant. A turning point for the field was the observation of oscillating peaks in the 2DES spectra of the FMO complex at 77 K, shown in the iconic image (Figure 11*a*) from Engel *et al.* (2007). The exciting observation was that the frequency of the oscillations matches the electronic energy gap between BChl *a* exciton bands in the FMO complex labeled exciton 1 and exciton 3 in Figure 8*b*, approximately 200 cm^{-1}. It hinted that this might be a discovery of electronic coherence that is remarkably resilient to decoherence.

The data suggested that the absorption bands of the these coupled chromophores were prepared in an initial superposition state by the broad-band pump pulses, then the superposition was 'read out' as a function of 'population time' delay by oscillations in the 2DES map. While such oscillations can be seen in broad-band femtosecond pump–probe experiments too (as we describe below), the significance of the 2DES experiment is that the way the oscillations are located in the 2DES map, and in the rephasing and non-rephasing decompositions of the map, aid assignment. The model calculation shown in Figure 11*b* shows that when we have electronic coherence in a two-level system, 2DES exhibits oscillations only in the cross-peaks of rephasing spectra and diagonal peaks of non-rephasing spectra (Branczyk *et al.*, 2014). We discuss this further below.

This result from Engel *et al.* (2007), thus strongly hinted that the 2DES experiment was visualizing electronic coherence in a complex biological system. What was most remarkable was the inexplicably

(a)

(b)

(c)
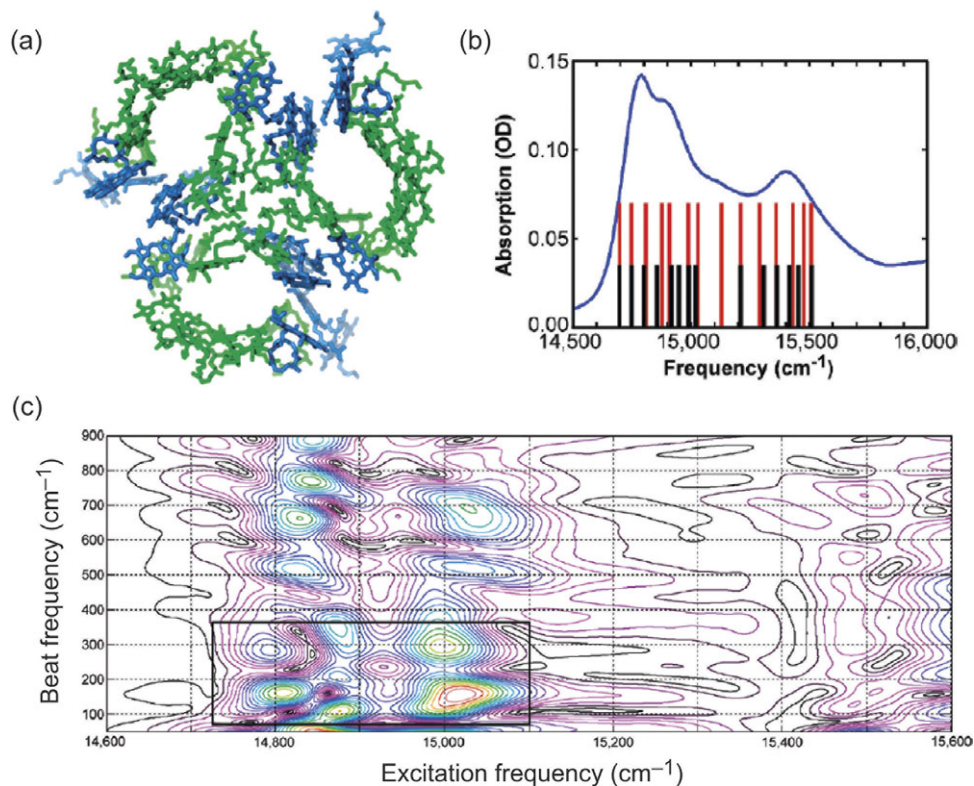
Figure 9. (a) Chl arrangement in LHCII trimer with Chl a and Chl b shown in green and blue, respectively. The phytyl chains have been omitted for clarity. (b) Linear absorption spectrum of LHCII trimers at 77 K. Red sticks indicate the exciton energies determined in this experiment, while black sticks are previously predicted values. (c) Power spectra of quantum beating in LHCII constructed from experimental 2DES data. Reprinted from (Calhoun *et al.* 2009) with permission. Copyright 2009 American Chemical Society.

(a) Relaxation Spectra   Nonrephasing Spectra   (b)

(c)
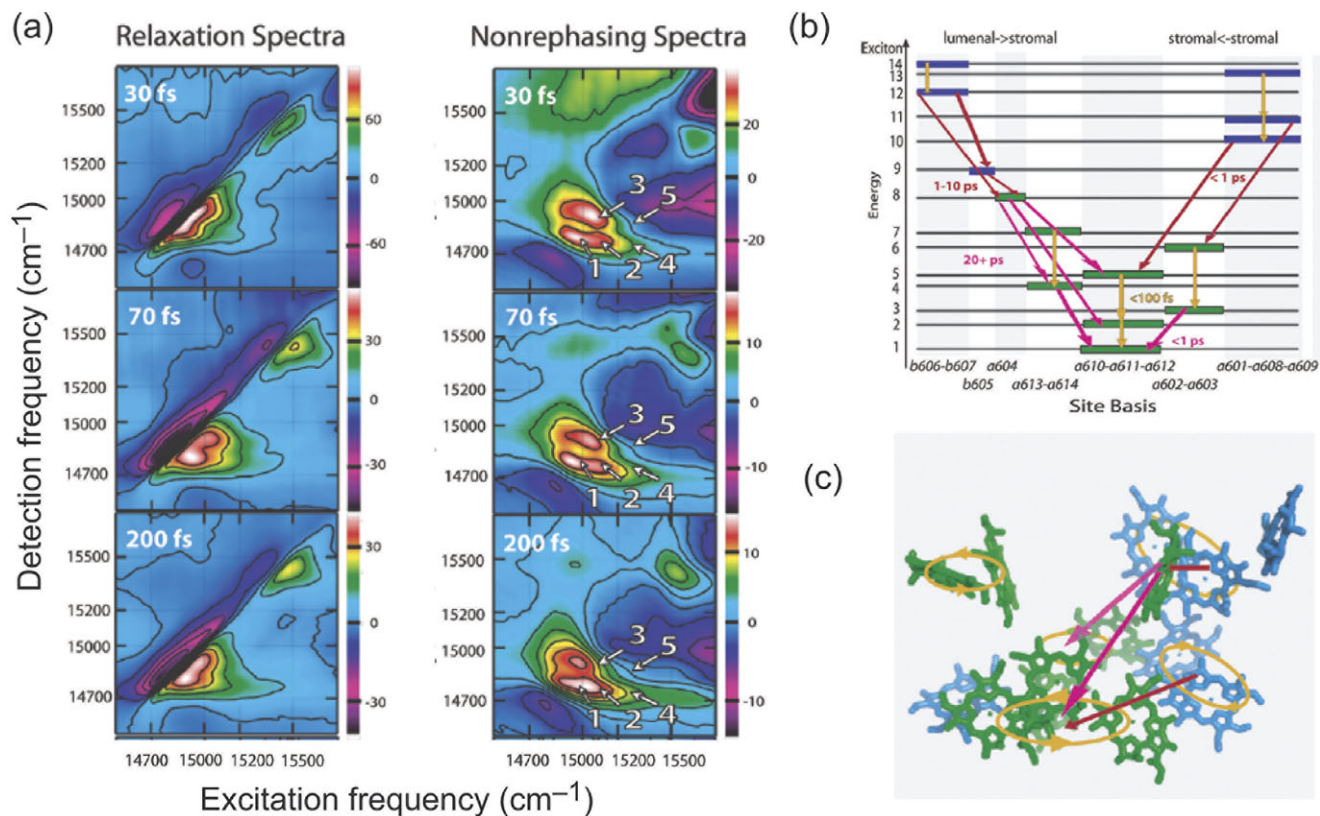
Figure 10. (a) Experimental real 2D relaxation (left) and nonrephasing (right) spectra of LHCII at 77 K for population times of 30, 70, 200, 300 fs, and 13 ps. Arrows point to cross-peaks on the nonrephasing spectra to highlight energy transfer dynamics. (b) Summary of the pathways of energy flow. The time scales indicate the approximate time at which the cross-peak signal corresponding to that pathway reaches its maximum. (c) Mapping of the energy flow pathways and exciton states onto the LHCII structure. Reprinted with permission from (Schlau-Cohen *et al.* 2009). Copyright 2009 American Chemical Society.
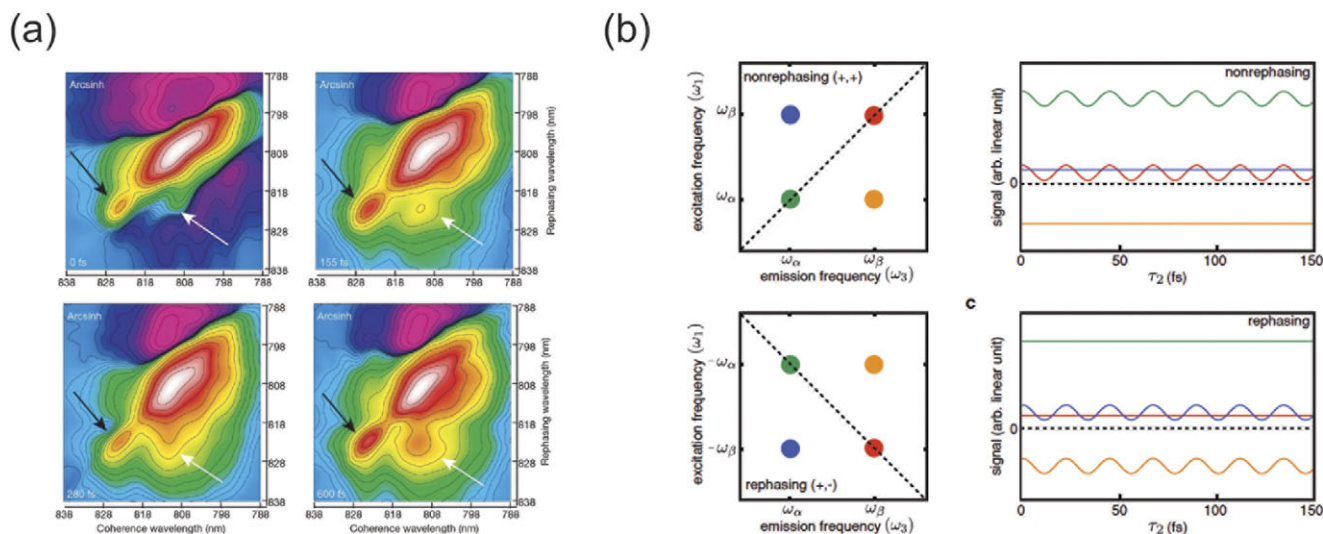
Figure 11. (a) Selected two-dimensional electronic spectra of the FMO complex are shown at population times from $T = 0$ to 600 fs demonstrating the emergence of the exciton 1–3 cross-peak (white arrows), amplitude oscillation of the exciton 1 diagonal peak (black arrows), the change in lowest-energy exciton peak shape and the oscillation of the 1–3 cross-peak amplitude. The data (Engel *et al.* 2007) are shown with an arcsinh coloration to highlight smaller features: amplitude increases from blue to white. Reprinted from (Engel *et al.* 2007) with permission. Copyright 2007 Springer Nature Limited. (b) Model calculations showing how, for an electronic coherence between two levels, 2DES exhibits oscillations on the cross-peaks of rephasing spectra and diagonal peaks of non-rephasing spectra. Reprinted with permission from (Branczyk *et al.* 2014). Copyright 2014 John Wiley and Sons.

slow dephasing time for this electronic coherence. Thus, debate and questions ensued regarding whether special properties of the protein somehow protected the electronic system from decoherence. The interesting questions and implications raised by the FMO experiments were the focus of an wide variety of conferences and workshops that ensued, including the inaugural Quantum Effects in Biological Systems workshop, held in Lisbon in 2009, and the 22nd Solvay Conference on Chemistry. An important concrete result of these interdisciplinary discussions was the understanding that 'noise', that is, disorder in energies, plays a key role in enabling efficient transport processes, epitomized by energy transfer in light harvesting (Caruso *et al.*, 2009; Rebentrost *et al.*, 2009a,b).

The experiments on the FMO complex were reproduced in other labs (Panitchayangkoon *et al.*, 2010; Hayes and Engel, 2011), but the detailed origin of the oscillations (see further discussion below) turned out to be more complicated than first thought. See also a review dedicated to this topic (Wang *et al.*, 2019). Nevertheless, the discovery, by inspiring a field of work, led remarkable leaps of insight into coherent EET dynamics and how to detect signatures of coherence.

Further work on this front used 2DES to examine an LHC, known as PC645, isolated from a bright cyan-colored cryptophyte algae (Figure 12a). A merit of studying PC645 is that the protein binds three different chromophores, each with a clear spectral signature. The bilin chromophores are color-coded in Figure 12a and the spectral positions of their absorption bands are displayed schematically under the experimental absorption spectra in Figure 12b. This picture also gives a clear account of how the 2DES spectra correlate the bands in the absorption spectra, displaying correlations via spectral cross-peaks. In these experiments, we noticed unusual coherent oscillations in the 2DES data measured for samples at room temperature (Collini *et al.*, 2010). They are similar to the coherences seen for the FMO complex, but with higher frequency (~700 cm^{-1}). We posited that this coherence could not be explained as simple vibrational wavepackets, as discussed below.

A particular significance of the oscillations in the FMO data and the PC645 data was that they showed the potential for 2DES spectroscopy to uncover dynamics of the system's density matrix. Measuring dynamics in the off-diagonal part of the density matrix can, in turn, unlock the possibility of detecting and characterizing quantum coherence – so this was a very exciting development. The reason that 2DES can shed light on the ultrafast time evolution of the density matrix is explained by the way the signal is generated systematically from a sequence of impulsive perturbations of the density matrix of the system (Mukamel, 1995; Cho *et al.*, 2005; Branczyk *et al.*, 2014). 2DES clearly has the potential to give relevant insights into the system's density matrix indirectly, but incisively resolving the density matrix directly remains an open question.

Our intuition is provided by representing the various ways the signal can be generated as double-sided Feynman diagrams. We will not go into detail here, but the important message is to catalog the ways that light–matter interactions can generate third-order nonlinear signals at the different pump–probe frequency coordinates in the 2DES map (Collini, 2021). An illustration of this idea is shown in Figure 12c (Scholes, 2010). The first light–matter interaction produces a coherence between the ground electronic state and the excited electronic state (β) of, for instance, the DBV($-$) state. The second light–matter interaction drives another absorption band (α), corresponding for instance to the PCB resonance. During the pump–probe (population) time delay we therefore see evolution of a coherence at a cross-peak between DBV($-$) and PCB. That coherence accumulates phase as a function of the pump–probe time delay, that is, the signal depends on $\omega_{\alpha\beta}t$ – thus producing oscillations in the cross-peak amplitude – just like we calculate by solving the time-dependent Schrödinger equation. We read out the oscillating signal in the prescribed cross-peak, allowing it to be identified to a particular double-sided Feynman diagram, like the one drawn.

The main evidence for the conclusion that some of the coherent oscillations observed in the 2DES experiments of PC645 came from very careful analysis of oscillations of the cross-peak in 2DES, specifically, comparing rephasing and non-rephasing spectra according to the strategy indicated in Figure 11b (Turner *et al.*, 2011, 2012). A vibrational coherence is expected to appear in *both* the rephasing and non-rephasing data (Mančal *et al.*, 2010; Nemeth *et al.*, 2010), typified by the 860 cm^{-1} (26 THz) oscillation indicated by the right-hand blue arrow in Figure 13b. In contrast, as noted in Figure 11b, an oscillation that comes primarily from electronic coherence should appear only in the cross-peaks of rephasing data,
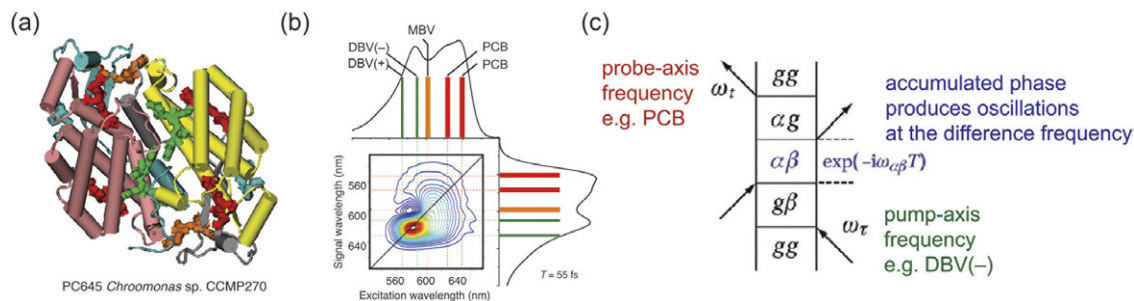
Figure 12. (a) Crystal structure of the PC645 LHC described in this work. The structure shows the different types of bound bilin chromohropes that we refer to in the text, specifically DBV (green) and PCB (red). (b) Depiction of a 2DES spectrum (298K) overlaid with the absorption spectrum of PC645 to emphasize how the spectral bands are resolved in the correlation map. (c) Example of a double-sided Feynman diagram that produces cross-peak oscillations.

like the 690 cm^{-1} (21 THz) oscillation indicated by the left-hand arrow (or the diagonal peaks in non-rephasing data). We emphasize again that it is this kind of analysis that makes 2DES such a key experiment – we can go beyond observing phenomena, such as coherent oscillations, to assigning their origin.

The analysis of 2DES data using the techniques described above is powerful, as long as the Born–Oppenheimer approximation holds. However, subsequent reports (Christensson et al., 2012; Chin et al., 2013; Plenio et al., 2013; Reimers et al., 2013; Tiwari et al., 2013) hypothesized that vibronic mixing between the vibrations and the excitons was behind the long-lived coherence. Vibronic mixing means that delocalized exciton-like states are formed by resonance between electronic transitions on one chromophore and an electronic plus vibrational transition on another (Reimers et al., 2015; Hestand and Spano, 2018); enabled by a level of theory beyond the usual Born–Oppenheimer approximation. Vibronic mixing obscures analyses of 2DES data that aim to distinguish electronic from vibrational coherence – essentially because the observed coherence involves both factors interplaying. This new insight therefore explains how coherences in 2DES can appear not to be simply vibrational wavepackets (Turner et al., 2012), yet they are inexplicably long-lived. Chin et al. (2013) provided the physical insight that vibronic coherences 'generate nonequilibrium processes that lead to the spontaneous creation and sustenance of electronic coherence, even at physiological temperatures'.

More recently, Cao et al. (2020) published a perspective of the vibronic coherences observed for photosynthetic LHCs and concluded that interexciton coherences are too short to have functional implications for light harvesting. Similarly, in another report, we struggled to identify a functional role for short-lived coherences (Scholes et al., 2017). Nevertheless, vibronic mixing, even if short-lived, can change the effective spectral overlap, and therefore rate, for 'downhill' EET (like in PC645; Dean et al., 2016), even though the ultrafast dynamics of EET are approximately incoherent (Blau et al., 2018; i.e., described reasonably well by a rate constant). This principle is the same as that indicated by the GFT model for EET, where the appropriate acceptor state is the delocalized (absorbing) exciton state (Scholes and Fleming, 2000), not the more localized equilibrium exciton state that is produced in less than 100 fs after photoexcitation. In the case of the short-lived acceptor state, recall that it enables B800 to B850 energy transfer to happen 10-fold faster than if the acceptor exciton were localized – a clear functional impact, even though the coherent state is very short-lived.

Experimental studies mostly support the hypothesis that the coherent oscillations are vibronic in origin (Maiuri et al., 2018; Thyrhaug et al., 2018). To give one intuitive example, the Blankenship group prepared FMO mutants where amino acids were altered in the protein scaffold that influence the spectra of BChl a

chromophores at the three and six positions (Maiuri et al., 2018) (Figure 14). Recall that the coherent oscillations of interest have a frequency of about 200 cm^{-1}, coinciding with the 190 cm^{-1} coherence seen in these very high signal-to-noise broad-band pump probe data. Recall also that the oscillation was assigned to arise from the exciton 1–3 coherence. Exciton 3 lies in the absorption spectrum just to the red of the 805 nm band (see Figure 8b), while exciton 2 is indicated here as the 813 nm band and exciton 1 is the 823 nm band.

For the Y16F mutant, the absorption band of exciton 1 is absent while changes to the excitonic structure higher in the absorption band are produced in the W184F mutant (likely affecting the exciton 3 band). It is therefore reasonable to expect that for the Y16F mutant in particular, we should not see the exciton 1–3 electronic coherence. However, both mutants showed exactly the same oscillations as the wild-type FMO complex. That observation suggests that we are measuring primarily vibrational coherences because the vibrations are intrinsic to the chromophores and are not affected by mutagenesis of the protein.

Nevertheless, it is notable that the 190 cm^{-1} vibrational coherence does match closely to the exciton 1–3 electronic frequency gap. This highlights the intriguing observation that vibrational frequencies in the FMO complex appear to be locked to excitonic energy gaps in the wild-type complex. It is remarkable that these resonances exist, and it is likely that they enhance spectral overlap. We see the same frequency matching between vibrational levels and electronic gaps in other LHCs, as well as photosystems (Romero et al., 2014). We give the compelling example of PC645 below.

Returning to the studies of PC645, the 2DES data allow correlations between the DBV 'emission' and PCB 'absorption' to be clearly resolved (Figure 15). We exploited the spectral features of PC645 to study the EET from the green chromophore DBV bands to the red chromophore PCB bands (Dean et al., 2016). That EET happens particularly fast, with a time constant of approximately 600 fs (Marin et al., 2011). Recall that there should be no correlations in the Förster limit. We focused on the oscillations that matched the DBV-PCB spectral gap, a huge 1,600 cm^{-1}. Like the FMO complex, this electronic gap (between two distinct chromophore types) is matched by a vibrational frequency. The correlations in the pattern of oscillations in the 2DES spectra are consistent with a vibronic coupling model, where the electronic states mix weakly via vibrational resonance (Figure 15b).

We postulated, on the basis of a vibronic coupling model for Förster-like spectral overlap, that this mixing can enhance the effective spectral overlap for EET by tuning Franck–Condon factors, and thus increase the rate of EET beyond what we would anticipate based on Förster theory.

Given the widespread interest in the results described here, it may be helpful to summarize. We started this section by the
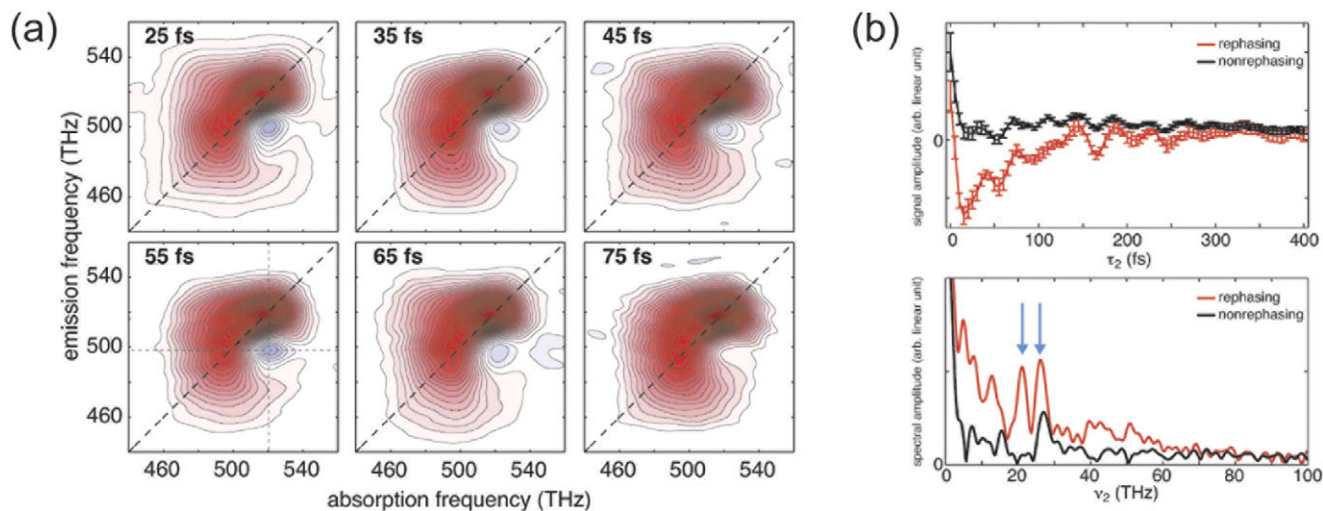
Figure 13. (a) Real part of the total 2DES signal for PC645 (ambient temperature) for several pump-probe delay times. Reproduced from (Turner *et al.* 2012) with permsission. Copyright 2012 Royal Society of Chemistry (Great Britain). The cross-peak being analyzed is indicated by the dashed lines. (b) Oscillations in the cross-peak. Reproduced from (Turner *et al.* 2011) with permission. Copyright the American Chemical Society 2011.
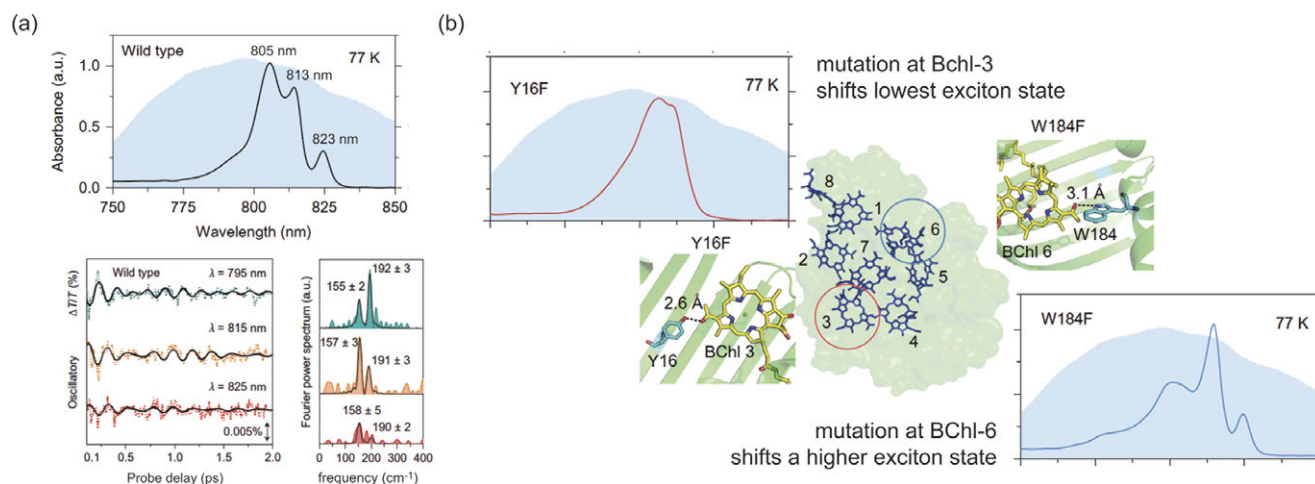
Figure 14. (a) Absorption spectra (77K) of the wild-type FMO complex, with wavelengths of the prominent bands (excitons 1, 2, 4) labeled. Analysis of broad-band pump-probe data reveals the coherent oscillations detected in the 2DES experiments, the coherence at 190 cm^{-1}, as well as a coherence at 155 cm^{-1}. (b) Mutant FMO complexes were prepared by mutagenesis of amino acids that affect absorption involving site 3 and site 6 BChls. Adapted from (Maiuri *et al.* 2018) with permission. Copyright Springer Nature Limited.

discovery of the 200 cm^{-1} coherence by Engel *et al.* (2007) in studies of the FMO protein from green sulfur bacteria at 77 K. The oscillations in the 2DES data were first thought to be electronic coherences, but a more careful analysis revealed these are vibronic wavepackets. Then we discussed the studies by Collini *et al.* (2010) of the cryptophyte PC645 LHC at ambient temperature, where detailed analysis of the oscillations in rephasing and non-rephasing 2DES spectra shows they cannot be explained as being purely vibrational wavepackets (Turner *et al.*, 2011). We then highlighted one of the follow-up studies of the oscillations seen after broad-band femtosecond excitation of the FMO complex. In those studies, mutagenesis allowed for compelling control experiments that reveal the vibrational wavepackets. These vibrational wavepackets lock to the 200 cm^{-1} electronic energy gap to give the vibronic coherence. Further 2DES experiments of the cryptophyte PC645 LHC showed that the shape of 'beat maps' evidence vibronic coherence, this time by locking a vibration and an electronic energy gap of 1,600 cm^{-1}. A key conclusion of all this work is that the matching of electronic and vibrational gaps in a variety of photo-synthetic systems is likely not a coincidence.

We have focused here on specific examples that we find helpful to illustrate the main findings. Of course, there has been intense activity in the field and many important papers. We refer the reader to this review (Wang *et al.*, 2019).

Development of improved theoretical descriptions of electronic energy transfer

EET is often described in one of two perturbative limits, but the insights from the experiments discussed above showed that to describe light harvesting quantitatively, we need a theory that interpolates between these limits (Ishizaki and Fleming, 2009a; Chenu and Scholes, 2015). The experiments inspired developments in this direction. We start by noting the limiting cases.

When the electronic coupling $\hbar J$ is small compared to the bath reorganization energy $\hbar\lambda$ (i.e., half the Stokes shift) and the electronic coupling can be described perturbatively, this is the domain of Förster theory as we have noted above. Just beyond this limit, when electronic coupling is still small, we can account for correlations in the donor emission and acceptor absorption that

(a)

PC645 *Chroomonas* sp. CCMP270

(b)

(c)

(d)
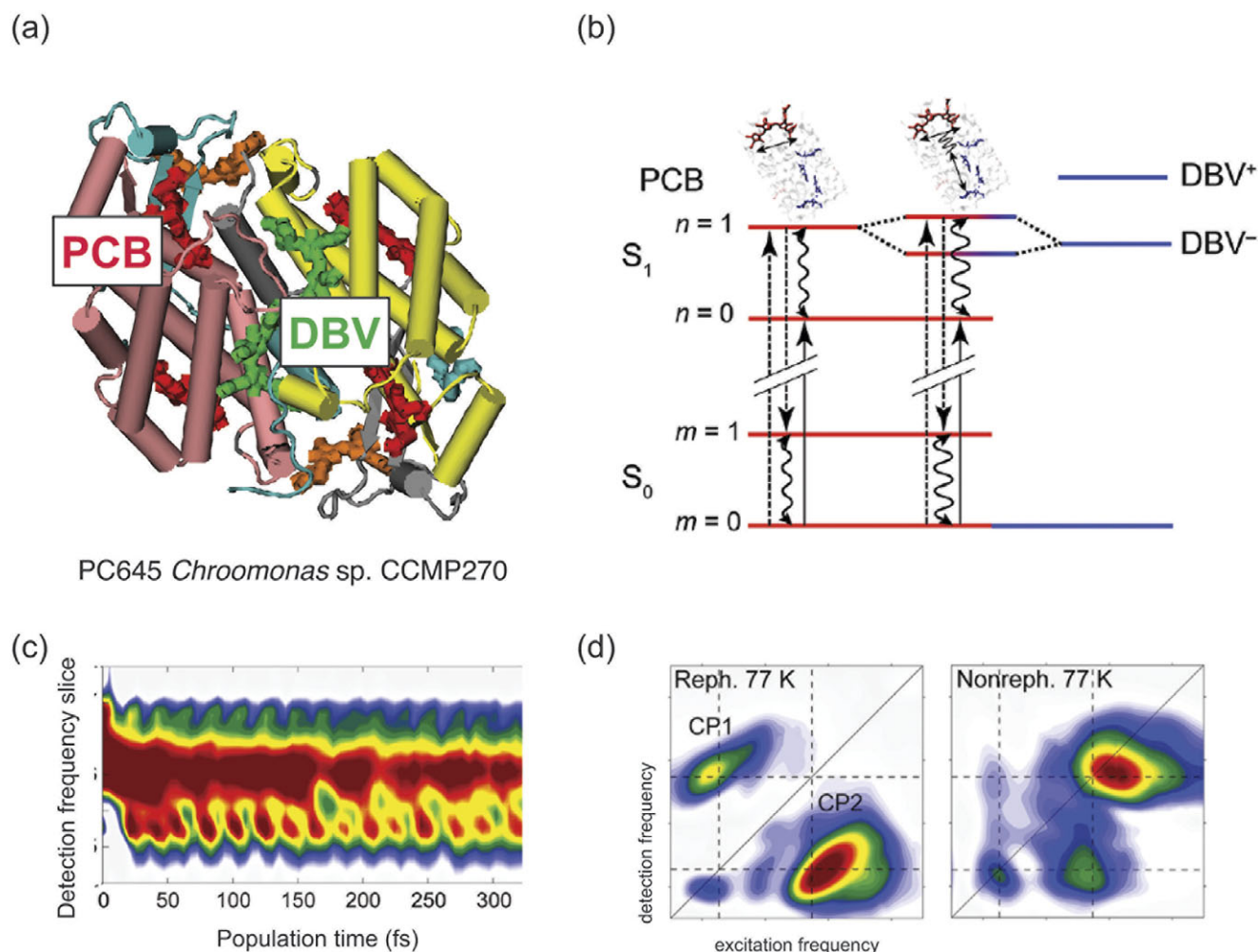
Figure 15. (a) Crystal structure of PC645 with the chromophores studied in these experiments labeled. (b) Model calculations of the vibronic exciton levels formed from mixing the 1,580 cm^{-1} vibrational coherence of PCB and the and DBV band. (c) 2DES data (77K) showing the oscillating cross-peak that indicates correlations between the DBV and PCB absorption bands. (d) Beat maps of the rephasing and non-rephasing 2DES data. Reproduced from (Dean *et al.* 2016) with permission. Copyright 2016 Elsevier.

transiently preserve donor–acceptor delocalization by wrapping up the spectral overlap and electronic coupling in a 'memory kernel' (Kenkre and Knox, 1974). In a multichromophoric generalization of Kenkre–Knox theory, we pick up interferences between energy transfer pathways and see that those interferences tend to be short-lived (Hossein-Nejad *et al.*, 2012). In the other limit, where the coupling of the electronic transitions to nuclear degrees of freedom is small, it is possible to treat that coupling perturbatively. This is the domain for which Redfield theory, originally developed for NMR, can be used. As is appropriate for NMR timescales, Redfield theory is a Markovian theory in which the environment relaxation timescale is assumed to be infinitely fast.

Redfield theory was taken up and applied to pump–probe studies of photosynthetic energy transfer by Leegwater (1996), Chachisvilis *et al.* (1997), Kühn and Sundström (1997), and Renger (2009). However, in traditional Redfield theory, all excitons and the ground state have the same potential energy surface. As the energy gap between two excitons increases, traditional Redfield theory calculation of the downhill relaxation rate shows a rapidly decreasing rate and does not coincide with the Förster theory result at large energy gaps (Ishizaki and Fleming, 2009a). Zhang *et al.* (1998) and Yang and Fleming (2002) introduced a modified form of Redfield theory which allows for displacement of the excitonic potential surfaces. Modified Redfield theory gives substantially faster

relaxation rates for electronic energy gaps on the order of, or larger than, the electronic coupling, J. In cases of large energy gaps, modified Redfield theory agrees with Förster theory, while in the opposite regime of small electron–phonon coupling and small excitonic gap, traditional and modified Redfield theory agree.

However, when the timescale of environmental reorganization, τ_{rel}, and the inverse of the electronic coupling J^{-1}, which, physically, is the time excitation needs to move from one pigment to another, become similar to each other, their relationship and interplay can become the key factors. This is the intermediate regime, described above, when $\lambda \sim J$ and or $\tau_{rel} \sim J$ which is the typical case for many photosynthetic systems. The challenge here is that there are no vanishingly small parameters, thus making standard perturbation and Markovian approaches inappropriate (Kimura *et al.*, 2000; Kimura and Kakitani, 2003).

To tackle predictions of EET in the intermediate coupling regime, Ishizaki and Fleming (2009b) demonstrated a non-Markovian approach to calculation of EET that describes quantum coherent wavelike motion and incoherent hopping in a unified manner. This approach is generally referred to as the hierarchy equations of motion or HEOM method and has become the benchmark for more approximate theoretical methods. The HEOM method reduces to Redfield theory and Förster theory in their respective limits of validity and, more importantly, it incorporates the 'difficult'

<table>
<tr><td>

Box 3. Answers to the questions raised in 1997.

In photosynthetic LHCs, the close chromophore spacing means that electronic couplings are not estimated accurately enough using the dipole approximation. Instead, we need to calculate the Coulombic coupling between *transition densities*.

When excitation energy moves on timescales comparable to, and interplaying with, energy gap correlations in spectral lineshapes, the dynamic Stokes shift, as well as changing delocalization of excitonic states – the intermediate coupling regime – a nonperturbative theory such as HEOM is required. Evidence suggests that in this regime excitation energy dynamics can be optimal by interplaying electronic delocalization with bath-induced localization.

The disordered energy landscape throughout light-harvesting complexes helps efficient and robust long-range energy transfer by creating multiple energy transfer pathways. This multiplicity of alternative pathways produces robustness.

The energy transfer dynamics in most photosynthetic LHCs is predominantly incoherent – that is, the energy jumps among sites or clusters of strongly interacting chromophores. Despite that overall conclusion, the details of the mechanism are not simply Förster-like, as evidenced in the 2DES experiments. Energy transfer occurs in the intermediate coupling regime. The key takeaway is that we have learned a lot about this difficult dynamical regime and, somewhat surprisingly, find that in the intermediate coupling regime energy transfer is best described as 'hopping-like'. Interference effects, while present, are relatively weak. Instead, the excited states – the stepping stones for the energy – are dynamic; they can be somewhat delocalized across molecules, but become more localized rapidly after excitation. So, an energy acceptor state presents a large spatial target which contracts after receiving the excitation.

</td></tr>
</table>

<table>
<tr><td>

Box 4. Features of two-dimensional electronic-vibrational spectra.

- Has spectral resolution along both excitation (electronic) and detection (vibrational) axes in contrast to visible pump-infrared probe spectra that only have resolution along the IR axis.
- All features are cross peaks, there is no diagonal signal.
- Spectral resolution of congested spectra is enhanced because the factors that spread out the frequencies along the two axes are generally unrelated and uncorrelated with each other.
- Energy transfer systems become increasingly symmetric with respect to the excitation axis with increasing waiting time.
- 2DEV spectra where the detection is in the mid-IR region do not, in general, exhibit lower frequency vibrational wavepackets.
- Because two different transition moments are involved, 2DEV spectra are very sensitive to vibronic coupling and to the mechanism of the vibronic coupling.
- Spectral features exhibit a time-dependent center line slope which relates to a cross-correlation between the vibrational dipole moment and the molecular dipole moment.

</td></tr>
</table>

Figure 16. The four third-order two-dimensional spectroscopies covering the vibrational and electronic excitation frequency ranges.

intermediate coupling regime. In the parameter region where coherent wavelike motion of excitation occurs, the HEOM method predicts the lifetime of coherence to be several times longer than that predicted by the Redfield approach. The HEOM method provided key insights into 2DES data because it consistently handles both the electronic dynamics (e.g., the development of cross peaks in the 2D spectrum) and the protein response to the dynamics (e.g., the shape of the diagonal peaks as waiting time, T, is increased).

The experiments highlighted above as pedagogical examples, as well as theoretical developments and other parallel work, helped answer most of the central questions posed in 1997. The state of the field 20 years after those questions were prominent is disclosed in Box 3. Notable was the significant advance in our understanding of coherence in energy transfer.
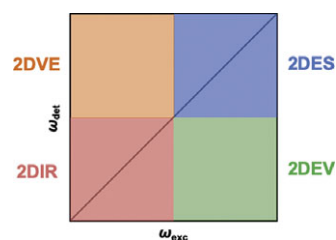
Origin and information content of two-dimensional electronic-vibrational (2DEV) spectra

The extensive debate triggered by our two *Nature* papers (Brixner *et al.*, 2005; Engel *et al.*, 2007) and by papers that followed rapidly from ScholesCollini *et al.* (2010) and Panitchayangkoon *et al.* (2010) inspired a large number of theoretical studies focusing on the origin of the oscillations glimpsed in Brixner *et al.* (2005) and observed so clearly in Engel *et al.* (2007). Despite much debate and a rough consensus that the long-lived beats were vibrational wave packets, and the shorter-lived ones possibly vibronic in origin, it seemed remarkable to me that no new types of experiments were aimed at resolving the problem, although a much-improved understanding of the cross-peak structure of 2D electronic spectra was developed (as described in a previous section).

In particular, it seemed that correlating the evolution of the nuclear degrees of freedom with that of the electronic structure would provide important new insight into the conspiracy of electrons and nuclei in chemical and biophysical dynamics. This led me to suggest to my group that we develop two-dimensional electronic-vibrational (2DEV) spectroscopy; the lower right quadrant in Figure 16. To put

this picture in perspective, note that the top right quadrant shows 2DES, while the lower left shows 2D infrared spectroscopy (2DIR). Box 4 summarizes key features of 2DEV spectroscopy (Arsenault *et al.*, 2021a; Arsenault and Fleming, 2022).

At first, this seemed a daunting prospect. It rapidly emerged that conventional phase-matching methods, as used in 2DES spectroscopy to isolate the desired signal, were not possible for 2DEV spectroscopy. When Tom Oliver arrived as a postdoc from Bristol University and Nick Lewis began as a graduate student, they teamed up to implement phase cycling to obtain the first 2DEV spectrum of a dye molecule undergoing solvation dynamics giving rise to its Stokes-shifted fluorescence. From my much earlier studies of solvation dynamics (Fleming *et al.*, 1998), I had always wondered how accurate the picture of a sudden change in dipole moment upon optical excitation, which then remained unchanged while the solvent accommodated to the new dipole, was in reality. In other words, is there feedback between the solvent and the molecule to synergistically enable further change in the dipole moment?

Indeed, this is what was found in our 2014 paper describing 2DEV spectroscopy (Oliver *et al.*, 2014). But we quickly realized that the domain of applicability of 2DEV spectroscopy was much broader than simple nonreactive systems – in particular, the highly congested spectra of photosynthetic Chl–protein complexes whose function is crucial to much of life on earth. In parallel with the development of 2DEV spectroscopy was a dramatic increase in the structural information available, largely through cryo-EM studies of the membrane proteins and their assemblies.

The first photosynthetic complex we studied by 2DEV spectroscopy (Lewis *et al.*, 2016) was the major LHC of vascular plants, LHCII, which forms trimers, each monomer of which contains eight Chl *a* and six Chl *b* molecules (Figure 9a). We were startled by the remarkable resolution of the 2DEV spectra given the broad Q_y region absorption spectrum with a shoulder marking Chl *b*
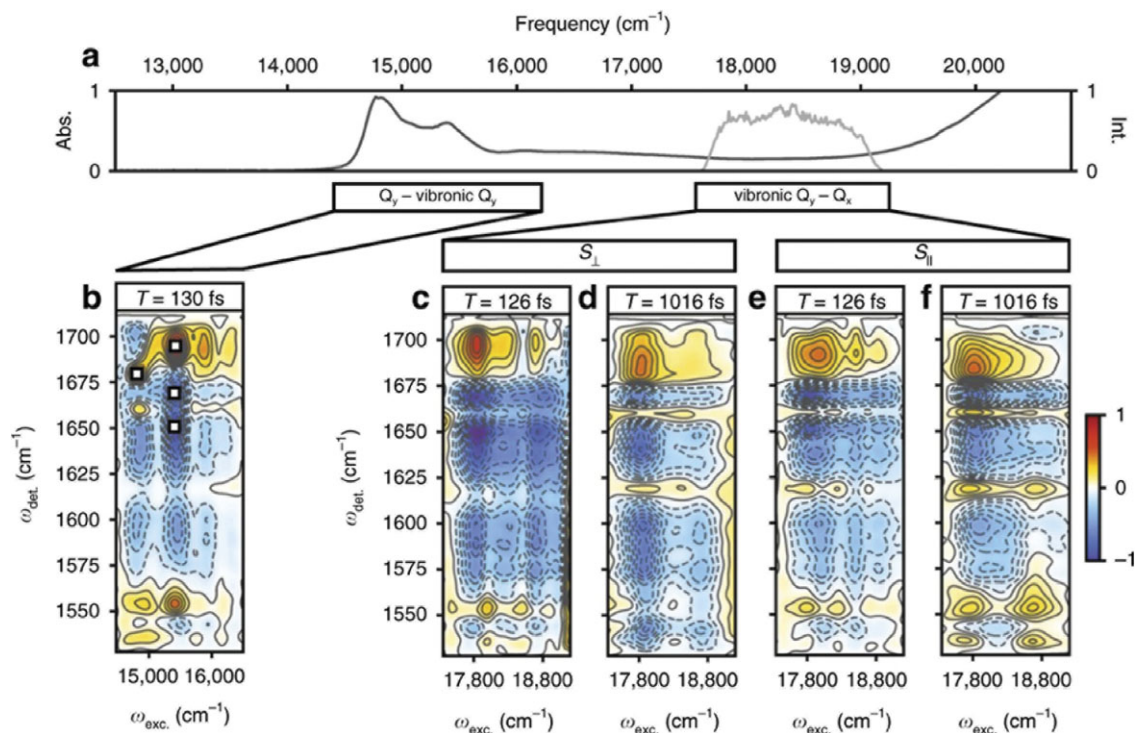
Figure 17. The electronic absorption spectrum and 2DEV spectra of the LHCII complex in the Q_y and Q_x regions. The laser spectrum for the Q_x region is also shown. Blue peaks represent excited state absorption and red peaks represent ground state bleaching. Adapted with permission from (Arsenault *et al.* 2020a).
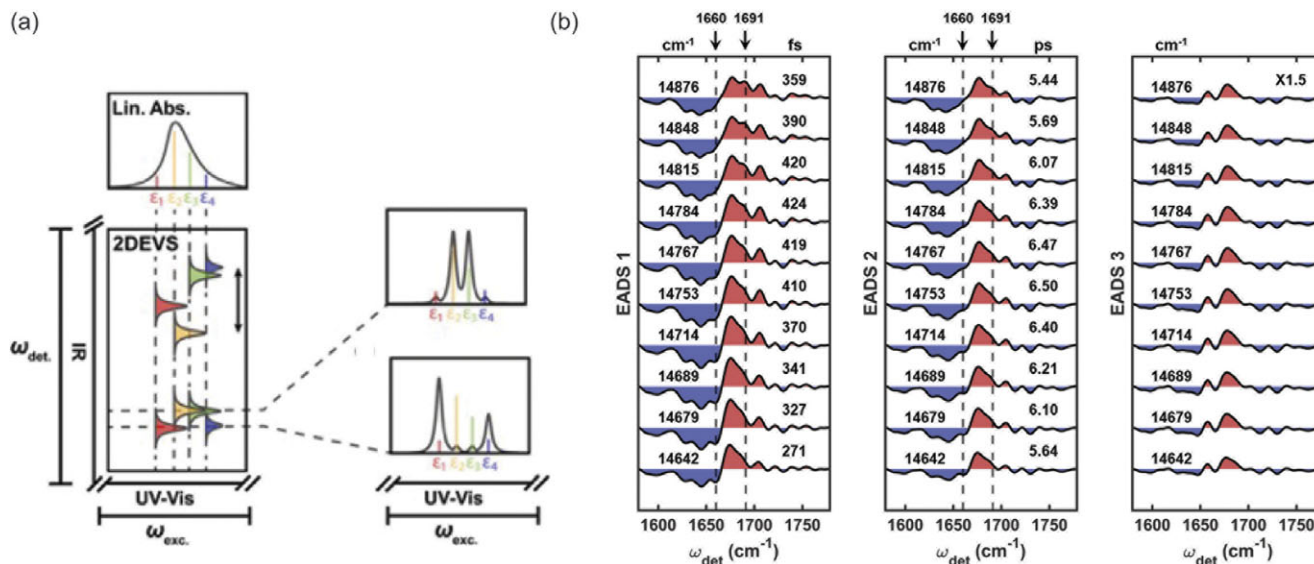

Figure 18. (a) 2DEV spectral resolution. (b) With the resolution along the excitation axis, we can perform global analysis at each individual excitation frequency with a simple sequential model. The vibrational structure in the EADS and the time constants will allow us to understand the spatial flow and kinetic nature of pathways. Reproduced with permission from (Yang *et al.* 2022). Copyright 2022 Europe PMC.

absorption, and the totally featureless Q_x region of the spectrum (Figure 17).

The spectral resolution evident in Figure 17 arises because the excitation (visible) and detection (infrared) frequencies are dispersed by unrelated and largely uncorrelated factors. As we have discussed, Coulomb coupling between the Chls produces excitons which are further spread out by site energy and chemical (Chl *a* and Chl *b*) differences. These differences are dramatized along the detection axis as vibrational frequencies are highly sensitive to local environments and charge states. This means that taking slices along

the excitation axis as a function of the IR frequencies can reveal remarkable detail. Figure 18*a* shows a cartoon of how the enhanced spectral resolution comes about, while Figure 18*b* shows actual data for the PSII core complex (Yang *et al.*, 2022).

So far, the 2DEV spectra have been discussed at an intuitive level. However, when multiple molecules are coupled electronically or vibronically, the appearance and evolution of the 2DEV spectrum is somewhat less intuitively obvious. To explore how spectra appear and evolve, first note that the appearance of a peak in a 2DEV spectrum requires that the conditional probability $P(\omega_e; \omega_v)$
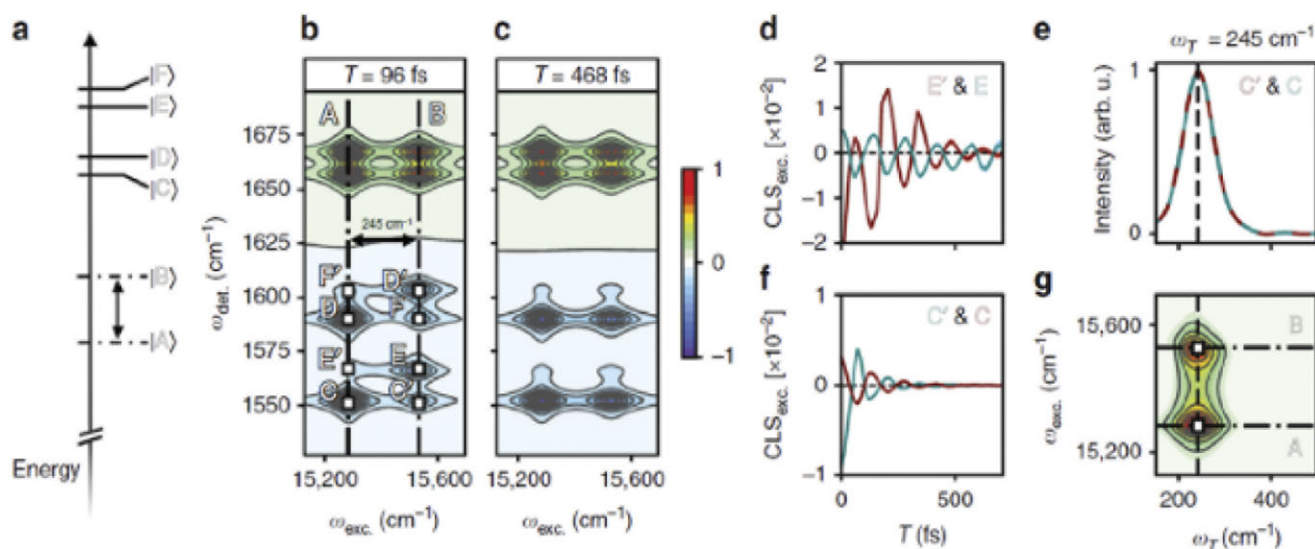
Figure 19. (a) Energy level diagram for the six excitonic states of the heterodimer model, where the ground state manifold has been omitted for clarity. b) and c) 2DEV spectra for the model at different waiting times. Positive features indicate ground state bleaches and negative features indicate excited state absorptions (ESAs). The two ESA quartets have been labeled as C, E, C′, and E′ and as D, F, D′, and F′. The two bands along the excitation axis have been marked by dashed-dotted black lines and labeled by the excitonic state that they originate from (A and B). The |B⟩- |A⟩ energy gap has also been labeled. d) and f) Center line slope dynamics along the excitation axis (CLS$_{exc.}$) of certain features, colored according to the peak labels in the top right corner of each plot. e) Magnitude of the cross-power spectrum of the CLSs of features C′ and C, where the oscillatory frequency of 245 cm^{-1} is marked by a dotted black line (a peak in the cross-power spectrum indicates a shared frequency). g) Intensity beat map along the excitation axis of features C′ and C, where the oscillatory frequency of 245 cm^{-1} is marked by a dotted black line and the involved excitation frequencies are labeled and marked by black dotted-dashed lines. Reproduced from (Arsenault *et al.* 2020b) with permission (http://creativecommons.org/licenses/by/4.0/).

is nonzero. In 2D electronic spectra, as we described above, the growth of cross-peaks as a result of, for example, EET where population flows from one state to another, and the interpretation of 2DES is intuitively clear. However, in 2DEV spectra, when EET occurs, the spectrum becomes increasing symmetric along the excitation axis as peaks corresponding to P(ω_{ed};ω_{vd}) begin to decay while peaks corresponding to P(ω_{ea};ω_{va}) gain amplitude (d, donor; a, acceptor) through the energy transfer (Lewis *et al.*, 2015).

In Arsenault *et al.* (2020b), we studied this feature of 2DEV spectra using a model of a coupled dimer, where each monomer (A and B) has one electronic and one vibrational degree of freedom. The coupling between A and B produces two excitons μ and ν. When the coupling is weak, the excitonic states are hardly mixed, and an excitation of an exciton ν, (mainly of B character), produces little if any vibrational features characteristic of A at short times. As the pump–probe (population) time *T* increases, the spectra become increasingly symmetric with new features characteristic of the lower electronic state, μ, appear. An important implication is that, because the vibrational motions are localized, they serve as spatial proxies allowing a mapping from the evolution in energy space to that in real space.

If the electronic coupling is strong, then the 2DEV spectrum of a vibronically mixed dimer becomes substantially more complex (Bhattacharyya and Fleming, 2019). For example, in general, IR transitions within one molecule will be much stronger than those that involve 'cross transitions' from one member of a coupled dimer to the other. But a resonant vibration can enable vibronic mixing between states localized on different monomers. In addition, optical transitions not evident in the electronic absorption spectrum can become prominent in a 2DEV spectrum via amplification through the IR transition moments. To date, no such strongly coupled photosynthetic systems have been studied by 2DEV spectroscopy. Possible examples are the special pair of purple bacterial RCs or perhaps the LH1 LHC of the same organisms.

Degenerate 2D spectroscopies such as 2DES give rise to line-shapes whose evolution is controlled by the dynamics of autocorrelation functions. The two different transition moments of 2DEV spectra, in contrast, lead to lineshapes reflecting cross-correlation functions. In the case of a single molecule, this cross-correlation is between the electronic and vibrational dipoles and reflects solvation dynamics and vibrational spectral diffusion (Cho and Fleming, 2020). We characterize this cross-correlation function by the center line slope (CLS) of the spectral features. In the case of coupled systems, insight is more readily achieved by numerical simulation of specific models. Figure 19 shows a model heterodimer system, each monomer having a single vibrational model, giving rise to six excitons (the ground state is omitted from the figure).

The coupling produces two ESA 'quartets', each with specific ratios of site character. As will be seen in the following section, these quartets are invaluable for the analysis of energy transfer in systems such as LHCs. The model shows increasing symmetry as waiting time increases – a characteristic of energy transfer. The center lines slopes are oscillatory (Figure 19*d,f*) which arises from the transfer between |A⟩ and |B⟩ excitons as made clear by the cross-power oscillation frequency matching the |A⟩ − |B⟩ energy gap of 245 cm^{-1} (Figure 19*e*) (Arsenault *et al.*, 2021b). The influence of vibronic coupling in 2DEV spectra was explored theoretically (Arsenault *et al.*, 2021b), then applied to LHCII. The results strongly suggested that Herzberg–Teller coupling (i.e., a nuclear dependence on the transition dipole coupling) plays a key role in facilitating energy transfer in LHCII (Arsenault *et al.*, 2021b,c).

Slices along the excitation axis at a specific detection frequency followed by Fourier transformation give a beat frequency map (Figure 19*g*) in which the correspondence of the beat frequency with the excitation frequency of the two components of the hetero-dimer is apparent. In multicomponent systems, the beat maps, although considerably more complex than that discussed in Figure 19, explicitly map which vibrational frequencies are involved in the relaxation of the excitons. It is important to note that we are not observing the coupled mode directly. The beats are observed in higher frequency, essentially local, vibrations through the modula-tion of the exciton energies by the lower frequency mode directly

involved in the coupling (mixing) of the two excitons. A second major advantage of the CLS, in comparison to the amplitude of cross peaks in 2DES, is that the CLS does not contain population dynamics. Rather, the CLS reports a correlation, making the extraction of beat frequencies more straightforward.

Applications of 2DEV spectroscopy for mapping energy flow in real space

2DEV spectroscopy, by focusing on the vibrational transactions in the final light–matter interaction, provides experimental input into the interplay of electronic and nuclear dynamics in ultrafast energy and charge transfer. A key advantage of this method is that, in many cases, the spectral dynamics do not contain any beats that are of purely vibrational origin. This allows the origin of beats that are observed to be distinguished and their role in the dynamics to become the focus. Finally, the CLS, as discussed above, contains unique information on the mixing and dynamics of specific levels. Beats in the CLS can be used to connect the energetic, spatial, and vibronic landscapes of pigment–protein complexes.

In Figure 20, we show 2DEV spectra of LHCII at four waiting times (Arsenault et al., 2020b). In the $T = 160$ fs data, eight specific features (four Chl a and four Chl b ESAs) are marked with white squares and labeled 1–8. In this review, we found the oscillatory behavior of the CLS for specific pairs, clearly indicating long-lived strongly oscillatory correlations (Arsenault et al., 2020b) between the electronic and nuclear degrees of freedom. By comparing the oscillatory frequencies of the CLS and the peak amplitudes of the 2DEV electronic excitation frequencies, we can read off which excitons are connected by a mode of the detected beat frequency as Figure 21 shows. By relating to the Hamiltonian of Novoderezhkin et al. (2005), the specific Chls involved can be clarified, completing the mapping of the evolution in energy space to one in real space.

2DEV spectroscopy has remarkably improved spectral resolution compared to other optical spectroscopies and retains femtosecond time resolution. This has enabled us to study energy flow in highly congested and increasingly large photosynthetic systems. For example, in the isolated PSII reaction center (PSII-RC), the unique IR signatures of different charged species allow us to identify the pigments involved in each step of charge separation – a topic of long-standing debate. In addition, resolution along the excitation axis allows separation of different pathways, reducing spectral congestion. Our results show that at longer excitation wavelengths, no energy transfer is needed to initiate charge separation, which proceeds from Chl_{D1} to $Pheo_{D1}$ in ~1 ps, followed by hole migration from Chl_{D1}^+ to $P_{D1}P_{D2}^+$ in ~6 ps (Yoneda et al., 2022). Our results agree with the multiscale simulations of Sirohiwal et al. (2020) and Sirohiwal and Pantazis (2023) in both mechanism and timescale. At shorter excitation wavelengths, the initial excitation is localized in $Chlz_{D1}$ and energy transfer to Chl_{D1} and $Pheo_{D1}$ (~40 ps) is required before charge separation can occur.

These results encouraged us to study progressively larger photosynthetic complexes, up to the PSII supercomplex (Figure 22). In the C_2S_2 form, the supercomplex contains 208 Chls, 156 of which are Chl a. Clearly, this poses a major challenge of data analysis, even with the added detail of the 2DEV spectra in both excitation and detection axes. For example, we found global analysis to have little value. We developed a full 208×208 rate matrix for our system via quantum dynamical calculations. Analyzing this model has the same issue – too much information. However, we can now carry out lifetime density analysis (LDA) (Leonardo et al., 2024) to create lifetime density maps (LDMs) on *both* the model and the data. The comparison of the two is aided by our and others' work on individual protein complexes, which enables us to pick out specific IR frequencies that are unique to individual complexes such as CP43 at 1,691 cm^{-1}. The consistency between the LDMs of the data and the model is excellent, mutually supporting one another.
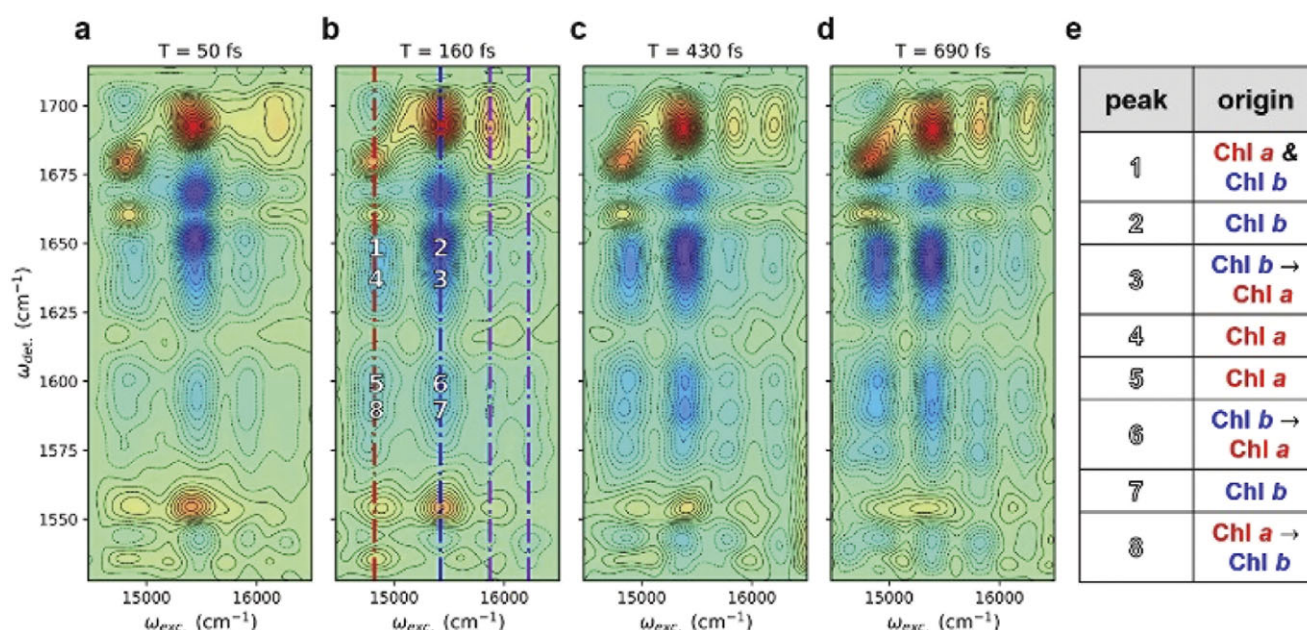
Figure 20. Two-dimensional electronic-vibrational spectra of LHCII at 77 K. a)–d) 2DEV spectra of LHCII at waiting times of T = 50, 160, 430, and 690 fs, respectively. The intensities of all spectra have been normalized to T = 0 fs. Red features outlined in solid contour lines indicate ground state bleaches and blue features outlined in dotted contour lines indicate excited state absorptions (ESAs). In b), ESA features of interest have been labeled, as well as the central locations of the predominantly Chl a excitonic band (red vertical line), predominantly Chl b excitonic band (blue vertical line), and higher-lying vibronic bands (purple vertical lines). e) Origins of peaks one through eight. Reproduced from (Arsenault et al. 2020b) with permission (http://creativecommons.org/licenses/by/4.0/).
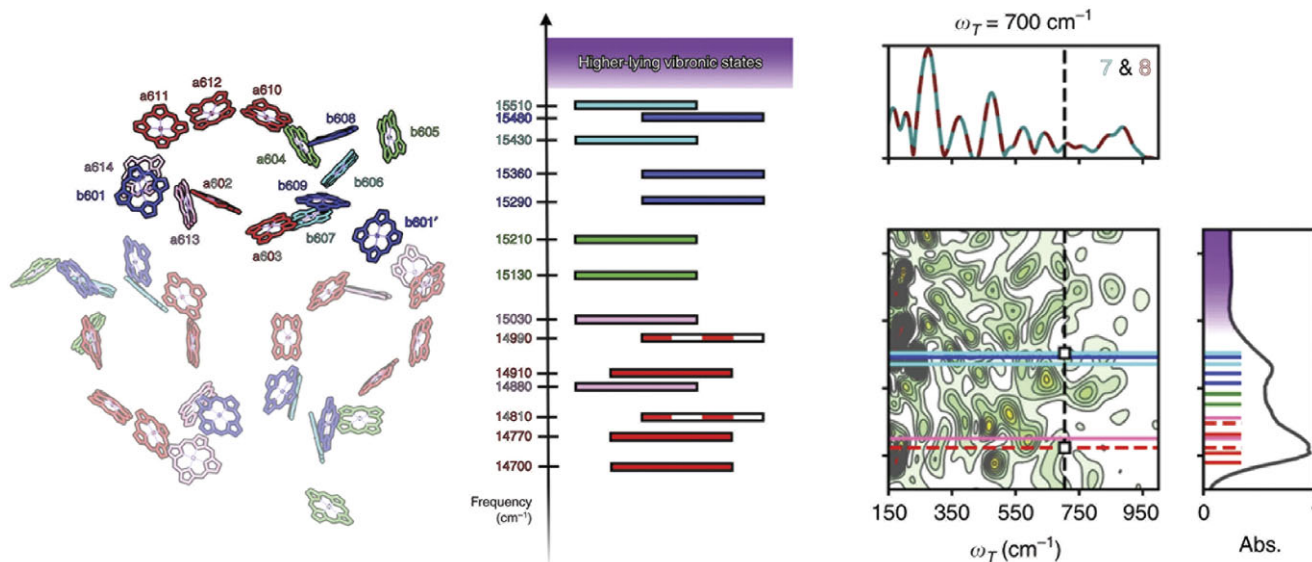
Figure 21. The Chl positions in an LHCII trimer along with the excitonic energy levels (center), and the cross-power spectrum between peaks labeled 7 and 8 (upper right) and the power spectra along the excitation axis at 1590 cm^{-1} (the detection frequency of features 7 and 8) (lower right). The horizontal lines indicate the excitons connected by the specific beat frequency highlighted (650 cm^{-1}). Reproduced from (Arsenault *et al.* 2020b) with permission (http://creativecommons.org/licenses/by/4.0/).
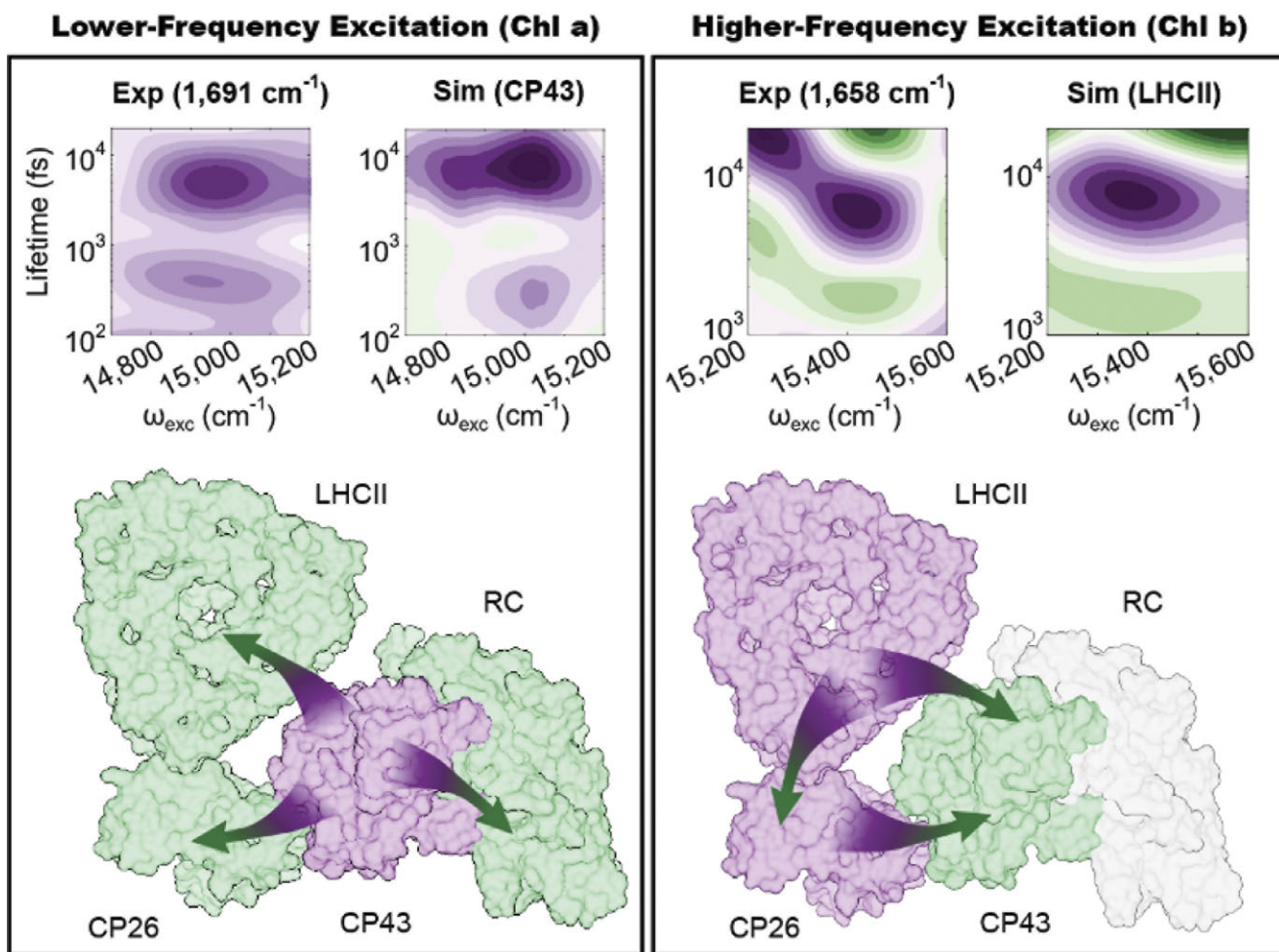
Figure 22. 2DEV experiment and simulations show that initially energy flows towards the peripheral antennae for Chl a excitation (left) and towards the PSII core for Chl b excitation (right). The bidirectional energy flow is crucial for balancing light-harvesting efficiency and photoprotection. Purple colors in the lifetime density maps indicate decays, green colors indicate growths. Adapted from Leonardo et al 2024 with permission. Copyright 2024 American Chemical Society.

Several remarkable conclusions follow: Excitation of complexes close to the RC results in faster energy transfer to the periphery than to the RC. In other words, excitation is most likely to leave the core and explore the peripheral antenna. In contrast, excitation in the Chl *b* spectral region of the peripheral LHCII complexes, leads to excitation moving through the peripheral antenna and toward the core (Leonardo *et al.*, 2024). The conclusion is that under certain initial conditions, PSII is an entropy-controlled system (a point we return to below) in which an excitation can explore the antenna system in a few 10s of ps. This reveals a potentially critical design principle in which an initial PSII excitation can explore potential quenching sites regardless of initial location, thus allowing both efficient light harvesting and effective photoprotection.

Conclusions and outlook

Overall, the work we have described here shows how development of new experimental methods can target questions of mechanism in ultrafast dynamics. This was a key step in moving away from simply timing processes, that is, resolving kinetics, to asking incisive questions about the theoretical models that underpin our understanding of the dynamics. It is especially encouraging that these kinds of experiments are feasible not only for simple model systems, but for biological systems of remarkable complexity. Through multidimensional spectroscopic methods combined with structural information and theory, we have revealed many of the design principles used by photosynthetic organisms to capture the sun's energy.

There have been many applications of 2DES to study other biological systems, ranging from studies of DNA photophysics in the ultraviolet to studies of bacteriorhodopsin, rhodopsin, and a variety of photosynthetic systems, as well as chemical systems and materials. For instance, considering only papers published so far this decade (2020–2023), there has been a compelling range of studies employing 2DES and developing 2DES experimental methods (Akhtar *et al.*, 2020, 2021, 2022; Li *et al.*, 2020; Palato *et al.*, 2020; Segarra-Martí *et al.*, 2020; Tran *et al.*, 2020; Tros *et al.*, 2020; Zuehlsdorff *et al.*, 2020; Son *et al.*, 2020b; Higgins *et al.*, 2021; Jun *et al.*, 2021; Mohan *et al.*, 2021; Mueller *et al.*, 2021; Russo *et al.*, 2021; Zhao *et al.*, 2021; Biswas *et al.*, 2022; Duan *et al.*, 2022; Ma *et al.*, 2022; Ross *et al.*, 2022; Roy *et al.*, 2022; Schultz *et al.*, 2022; Timmer *et al.*, 2022; Kim *et al.*, 2022b; Brosseau *et al.*, 2023; Fisher *et al.*, 2023; Jana *et al.*, 2023; Jeffries *et al.*, 2023; Lee *et al.*, 2023; Liu *et al.*, 2023; Lüttig *et al.*, 2023; Rojas-Gatjens *et al.*, 2023; Nguyen *et al.*, 2023b). What is especially notable about this list of recent literature is that 2DES now has found many applications for the study of chemical materials. That has been partly motivated by the way 2DES can disentangle complicated spectra. Further, 2DES has been useful for identifying the nature of complex excited state species that are produced through the interplay of delocalization, charge separation, and lattice distortion.

2DEV spectroscopy, being a newer method, has a smaller number of applications (Gaynor *et al.*, 2021; Song *et al.*, 2021a,b; Nguyen *et al.*, 2023a) and theoretical development (Gaynor *et al.*, 2021; Song *et al.*, 2021a; Weakly *et al.*, 2021; Polley and Loring, 2022; Nguyen *et al.*, 2023a; Zhang *et al.*, 2023) in the current decade.

Thinking about the topics covered in this review, we will describe here three major conclusions and how they inform needs for future research.

The first conclusion concerns energy flow pathways and dynamics. In the 2DES experiments, we learned much about ultrafast dynamics of energy transfer over domains comprising 6 to 20 or so chromophores. 2DEV experiments showed that surprising detail can even be resolved on much larger complexes. But photosynthesis starts with energy migration through even larger landscapes of chromophores, and the excitation is eventually trapped in the photosystems (or quenched by a regulation apparatus). How can we obtain 'pictures' of these large-scale and complex trajectories of dynamics in such a way that we can depict how the initial reactions in photosynthesis work as a *system*? What experiments are needed and what precisely do we need to resolve – that is, how shall we depict function of the system with sufficient resolution and detail that we can elucidate how the function emerges (nonlinearly) from interplay of the interacting components?

For example, the $C_2S_2M_2$ PSII supercomplex contains 308 Chls and 24 subunits. What are the functions of all these subunits? PSII is the most rapidly dismantled, repaired, and reassembled complex known, so a multi-subunit design is clearly valuable. This also enables the modulation of antenna size in conditions of ample sunlight, for example. Yet, the fact that there are five different subunits in the core antenna, for example, is striking. A key to defining the roles of, say, CP43 and CP47 comes from modeling the dynamics and constructing first passage time (FPT) distributions to the RC (Yang et al, 2024). How can we define the dominant trajectories from light absorption to sensitization of the RC? Can such trajectories be observed experimentally?

While experimentally measuring exciton diffusion lengths is possible, elucidating FPT distributions is much more challenging, despite FPT to the RC being a key component that allows PSII to achieve energy regulation through entropy control. Will higher-order nonlinear spectroscopies become as impactful as the third-order spectroscopies described in the present article, now that Malý *et al.* (2023) have shown how to separate the orders of the nonlinear response so cleanly and simply? For example, can we learn about trajectories from the fifth-order (two-particle) response? Simulation can bridge diffusion length measurements and FPT distributions. In particular, it can be combined with machine learning, as the analytical relationship between diffusion lengths and FPT distributions is difficult to obtain due to complexity of the energy transfer network. If a machine is properly trained, a prediction of FPT distributions can be made from the experimentally obtained exciton diffusion lengths. Such an ability should provide critical insight into the working mechanism of entropy-controlled dynamics in PSII and should facilitate the design of controllable solar energy devices.

The second conclusion relates to the theme of the review – step-changes in our understanding can be driven by devising an experiment that addresses mechanism. What are the next kinds of experiments needed?

The third conclusion is that multidimensional spectroscopy provides a way to detect and characterize coherences. The studies discussed in this review yielded evidence for surprising vibronic coherences in photosynthetic complexes. Pure electronic coherences are more difficult to measure because molecular spectra contain many vibrational states. Nevertheless, clear electronic coherences have been detected in inorganic systems (Cassette *et al.*, 2014).

One tantalizing open issue concerns coherence: can an incoherently excited system generate coherence through its own dynamics? It may not be possible to settle this question with classical light pulses and methods. Photon statistics, in particular, the second-

order quantum coherence function $g^2(\tau)$, has been proposed as a way to address this issue (Holdaway *et al.*, 2018; Sánchez Muñoz and Schlawin, 2020). More recently, Olaya-Castro has developed the theoretical basis for interpreting $g^2(\tau)$ when no initial coherence is present in, for example, a LHC (Nation *et al.*, 2024). Initial proposals by Sánchez Muñoz and Schlawin (2020) suggested that two-color $g^2(0)$ may be adequate to settle the issue of 'intrinsic' coherence. However, Olaya-Castro's recent work shows that the full $g^2(\tau)$ is actually required. Measuring $g^2(\tau)$ with adequate time resolution is a daunting task, but this appears to be a crucial future experiment to attempt.

Another open question that emerged from this work is whether nonclassical (quantum) correlations can enable function or properties in very complex systems – chemical systems or biological systems. What is needed is an experiment that can measure nonclassical correlations in really complex systems. An example is to be able to ask what properties do delocalized molecular exciton states have that could not be exhibited by a classical coherent state? Then, how can these states provide a resource for some kind of function? (Box 5).

References

Abramavicius D and Mukamel S (2004) Many-body approaches for simulating coherent nonlinear spectroscopies of electronic and vibrational excitons. *Chemical Reviews* **104**, 2073–2098.

Abramavicius D, Palmieri B, Voronine DV, Sanda F and Mukamel S (2009) Coherent multidimensional optical spectroscopy of excitons in molecular aggregates; quasiparticle versus supermolecule perspectives. *Chemical Reviews* **109**, 2350–2408.

Akhtar P, Caspy I, Nowakowski PJ, Malavath T, Nelson N, Tan HS and Lambrev PH (2021) Two-dimensional electronic spectroscopy of a minimal photosystem I complex reveals the rate of primary charge separation. *Journal of the American Chemical Society* **143**(36), 14601–14612. https://doi.org/10.1021/jacs.1c05010.

Akhtar P, Nowakowski PJ, Wang WD, Do TN, Zhao SH, Siligardi G, Garab G, Shen JR, Tan HS and Lambrev PH (2020) Spectral tuning of light-harvesting complex II in the siphonous alga *Bryopsis corticulans* and its effect on energy transfer dynamics. *Biochimica et Biophysica Acta-Bioenergetics* **1861**(7), 148191. https://doi.org/10.1016/j.bbabio.2020.148191.

Akhtar P, Sipka G, Han WH, Li XY, Han GY, Shen JR, Garab G, Tan HS and Lambrev PH (2022) Ultrafast excitation quenching by the oxidized photosystem II reaction center. *Journal of Chemical Physics* **156**(14), 145101. https://doi.org/10.1063/5.0086046.

Arnold W and Oppenheimer JR (1950) Internal conversion in the photosynthetic mechanism of blue-green algae. *Journal of General Physiology* **33**(4), 423–435. https://doi.org/10.1085/jgp.33.4.423.

Arsenault EA, Bhattacharyya P, Yoneda Y and Fleming G (2021a) Two-dimensional electronic-vibrational spectroscopy: Exploring the interplay between electrons and nuclei in excited state dynamics. *Journal of Chemical Physics* **155**, 020901.

Arsenault EA and Fleming GR (2022) Two-dimensional electronic vibrational spectroscopy of complex molecular systems. In Pullerits T (ed.), *Nobel Symposium 173 Exploring Complex Molecular and Condensed Phase Processes and Functions by Multidimensional Spectroscopy from THz to X-Rays*. Båstad, Sweden.

Arsenault EA, Schile AJ, Limmer DT and Fleming G (2021b) Vibronic coupling and two-dimensional electronic-vibrational spectra. *Journal of Chemical Physics* **155**, 054201.

Arsenault EA, Schile AJ, Limmer DT and Fleming GR (2021c) Vibronic coupling in light harvesting complex II revisited. *Journal of Chemical Physics* **155**, 096101.

Arsenault EA, Yoneda Y, Iwai M, Niyogi KK and Fleming GR (2020a) The role of mixed vibronic Q_y-Q_x states in green light absorption of light-harvesting complex II. *Nature Communications* **11**(1), 6011. https://doi.org/10.1038/s41467-020-19800-y.

Arsenault EA, Yoneda Y, Iwai M, Niyogi KK and Fleming GR (2020b) Vibronic mixing enables ultrafast energy flow in light-harvesting complex II. *Nature Communications* **11**(1), 1460. https://doi.org/10.1038/s41467-020-14970-1.

Bhattacharyya P and Fleming GR (2019) Two-dimensional electronic-vibrational spectroscopy of coupled molecular complexes: A near-analytical approach. *Journal of Physical Chemistry Letters* **10**(9), 2081−2089. https://doi.org/10.1021/acs.jpclett.9b00588.

Biswas S, Kim J, Zhang X and Scholes GD (2022) Coherent two-dimensional and broadband electronic spectroscopies. *Chemical Reviews* **122**, 4257–4321.

Björn LO and Govindjee (2009) The evolution of photosynthesis and chloroplasts. *Current Science* **96**, 1466–1474.

Blankenship RE (2021) *Molecular Mechanisms of Photosynthesis*, 3rd ed. - New York: Wiley.

Blau SM, Bennett DIG, Kreisbeck C, Scholes GD and Aspuru-Guzik A (2018) Local protein solvation drives direct down-conversion in phycobiliprotein PC645 via incoherent vibronic transport. *Proceedings of the National Academy of Science United States of America* **115**, E3342–E3350. https://doi.org/10.1073/pnas.1800370115.

Branczyk A, Turner DB and Scholes GD (2014) Crossing disciplines – A view on two-dimensional optical spectroscopy. *Annalen Physik* **526**, 31–49.

Brixner T, Mancal T, Stiopkin IV and Fleming GR (2004) Phase-stabilized two-dimensional electronic spectroscopy. *Journal of Chemical Physics* **121**(9), 4221–4236. https://doi.org/10.1063/1.1776112.

Brixner T, **Stenger J**, **Vaswani HM**, **Cho M**, **Blankenship RE and Fleming GR** (2005) Two-dimensional spectroscopy of electronic couplings in photosynthesis. *Nature* **434**, 625–628.

Brosseau P, **Ghosh A**, **Seiler H**, **Strandell D and Kambhampati P** (2023) Exciton-polaron interactions in metal halide perovskite nanocrystals revealed via two-dimensional electronic spectroscopy. *Journal of Chemical Physics* **159**(18), 184711. https://doi.org/10.1063/5.0173369.

Calhoun TR, **Ginsberg NS**, **Schlau-Cohen GS**, **Cheng Y-C**, **Ballottari M**, **Bassi R and Fleming GR** (2009) Quantum coherence enabled determination of the energy landscape in light-harvesting complex II. *Journal of Physical Chemistry B* **113**, 16291–16295.

Cao JS, **Cogdell RJ**, **Coker DF**, **Duan HG**, **Hauer J**, **Kleinekathöfer U**, **Jansen TLC**, **Mancal T**, **Miller RJD**, **Ogilvie JP**, **Prokhorenko VI**, **Renger T**, **Tan HS**, **Tempelaar R**, **Thorwart M**, **Thyrhaug E**, **Westenhoff S and Zigmantas D** (2020) Quantum biology revisited. *Science Advances* **6**(14), eaaz4888. https://doi.org/10.1126/sciadv.aaz4888.

Caruso F, **Chin AW**, **Datta A**, **Huelga SF and Plenio MB** (2009) Entanglement and entangling power of the dynamics in light-harvesting complexes. *Journal of Chemical Physics* **131**, 105106.

Cassette E, **Pensack RD**, **Mahler B and Scholes GD** (2014) Room-temperature exciton coherence and dephasing in two-dimensional nanostructures. *Nature Communications*, **6**, 6086.

Chachisvilis M, **Kühn O**, **Pullerits T and Sundström V** (1997) Excitons in photosynthetic purple bacteria: Wavelike motion or incoherent hopping? *Journal of Physical Chemistry B* **101**, 7275–7283.

Chenu A and Scholes GD (2015) Coherence in energy transfer and photosynthesis. *Annual Reviews of Physical Chemistry* **66**, 69–96.

Chin AW, **Prior J**, **Rosenbach R**, **Caycedo-Soler F**, **Huelga SF and Plenio MB** (2013) The role of non-equilibrium vibrational structures in electronic coherence and recoherence in pigment–protein complexes. *Nature Physics* **9**, 113–118.

Cho M (2008) Coherent two-dimensional optical spectroscopy. *Chemical Reviews* **108**, 1331–1418.

Cho M and Fleming GR (1996) Chromophore-solvent dynamics. *Annual Reviews of Physical Chemistry* **47**, 109–134.

Cho M and Fleming GR (2020) Two-dimensional electronic-vibrational spectroscopy reveals cross-correlation between solvation dynamics and vibrational spectral diffusion. *Journal of Physical Chemistry B* **124**(49), 11222–11235. https://doi.org/10.1021/acs.jpcb.0c08959.

Cho MH, **Vaswani HM**, **Brixner T**, **Stenger J and Fleming GR** (2005) Exciton analysis in 2D electronic spectroscopy. *Journal of Physical Chemistry B* **109**, 10542–10556.

Christensson N, **Kauffmann HF**, **Pullerits T and Mancal T** (2012) Origin of long-lived coherences in light-harvesting complexes. *Journal of Physical Chemistry B* **116**, 7449–7454.

Cogdell RJ, **Gall A and Köhler J** (2006) The architecture and function of the light-harvesting apparatus of purple bacteria: From single molecules to in vivo membranes. *Quarterly Reviews of Biophysics* **39**, 227–324.

Collini E (2021) 2D electronic spectroscopic techniques for quantum technology applications. *Journal of Physical Chemistry C* **125**, 13096–13108.

Collini E, **Wong CY**, **Wilk KE**, **Curmi PMG**, **Brumer P and Scholes GD** (2010) Coherently wired light-harvesting in photosynthetic marine algae at ambient temperature. *Nature* **463**, 644–648.

Croce R and van Amerongen H (2014) Natural strategies for photosynthetic light harvesting. *Nature Chemical Biology* **10**, 492–501.

Curutchet C, **Kongsted J**, **Munoz-Losa A**, **Hossein-Nejad H**, **Scholes GD and Mennucci B** (2011) Photosynthetic light-harvesting is tuned by the heterogeneous polarizable environment of the protein. *Journal of the American Chemical Society* **133**, 3078–3084.

Curutchet C and Mennucci B (2005) Toward a molecular scale interpretation of excitation energy transfer in solvated bichromophoric systems. *Journal of the American Chemical Society* **127**(47), 16733–16744. https://doi.org/10.1021/ja055489g.

Curutchet C and Mennucci B (2017) Quantum chemical studies of light harvesting. *Chemical Reviews* **117**, 294–343.

Curutchet C, **Scholes GD**, **Mennucci B and Cammi R** (2007) How solvent controls electronic energy transfer and light harvesting: Toward a quantum-mechanical description of reaction field and screening effects. *Journal of Physical Chemistry B* **111**(46), 13253–13265. https://doi.org/10.1021/jp075411h.

Dahlberg PD, **Fidler AF**, **Caram JR**, **Long PD and Engel GS** (2013) Energy transfer observed in live cells using two-dimensional electronic spectroscopy. *Journal of Physical Chemistry Letters* **4**(21), 3636–3640. https://doi.org/10.1021/jz401944q.

Dean J, **Mirkovic T**, **Toa Z**, **Oblinsky D and Scholes GD** (2016) Vibronic enhancement of algae light harvesting. *Chem* **1**, 858–872.

Dean J and Scholes GD (2017) Coherence spectroscopy in the condensed phase: Insights into molecular structure, environment, and interactions. *Accounts of Chemical Research* **50**, 2746–2755.

Deisenhofer J and Michel H (2004) The photosynthetic reaction centre from the purple bacterium *Rhodopseudomonas viridis*. *Bioscience Reports* **24**, 323–361.

Dostál J, **Psencík J and Zigmantas D** (2016) *In situ* mapping of the energy flow through the entire photosynthetic apparatus. *Nature Chemistry* **8**(7), 705–710. https://doi.org/10.1038/nchem.2525.

Du M, **Xie X**, **Mets L and Fleming GR** (1994) Direct observation of ultrafast energy-transfer processes in light-harvesting complex-II. *Journal of Physical Chemistry* **98**, 4736–4741.

Duan HG, **Jha A**, **Chen LP**, **Tiwari V**, **Cogdell RJ**, **Ashraf K**, **Prokhorenko VI**, **Thorwart M and Miller RJD** (2022) Quantum coherent energy transport in the Fenna–Matthews–Olson complex at low temperature. *Proceedings of the National Academy of Sciences of the United States of America* **119**(49), e2211630119. https://doi.org/10.1073/pnas.2107266119.

Duysens LNM (1951) Transfer of light energy within the pigment systems present in photosynthesizing cells. *Nature* **168**, 548–550.

Duysens LNM (1964) Photosynthesis. *Progress in Biophysics and Molecular Biology* **14**, 1–104.

Engel GS, **Calhoun TR**, **Read EL**, **Ahn T-K**, **Mancal T**, **Cheng Y-C**, **Blankenship RE and Fleming GR** (2007) Evidence for wavelike energy transfer through quantum coherence in photosynthetic systems. *Nature* **446**, 782–786.

Fidder H, **Knoester J and Wiersma DA** (1991) Optical properties of disorder molecular aggregates: A numerical study. *Journal of Chemical Physics* **95**, 7880–7890.

Fidler AF, **Singh VP**, **Long PD**, **Dahlberg PD and Engel GS** (2013) Probing energy transfer events in the light harvesting complex 2 (LH2) of *Rhodobacter sphaeroides* with two-dimensional spectroscopy. *Journal of Chemical Physics* **139**(15), 155101. https://doi.org/10.1063/1.4824637.

Fidler AF, **Singh VP**, **Long PD**, **Dahlberg PD and Engel GS** (2014) Dynamic localization of electronic excitation in photosynthetic complexes revealed with chiral two-dimensional spectroscopy. *Nature Communications* **5**, 3286. https://doi.org/10.1038/ncomms4286.

Fisher JM, **O'Connor JP**, **Brown PJ**, **Kim T**, **Lorenzo ER**, **Young RM and Wasielewski MR** (2023) Two-dimensional electronic spectroscopy reveals vibrational modes coupled to charge transfer in a julolidine-BODIPY dyad. *Journal of Physical Chemistry A* **127**(13), 2946–2957. https://doi.org/10.1021/acs.jpca.3c01122.

Fleming GR, **Passino SA and Nagasawa Y** (1998) The interaction of solutes with their environments. *Philosophical Transactions of the Royal Society of London Series A* **356**, 389–404.

Fleming GR and Phillips D (2004) George Porter KT OM, Lord Porter of Luddenham 6 December 1920 - 31 August 2002. *Biographical Memoirs of Fellows of the Royal Society* **50**, 257–283.

Fleming GR and van Grondelle R (1997) Femtosecond spectroscopy of photosynthetic light-harvesting systems. *Current Opinions in Structural Biology* **7**, 738–748.

Förster T (1965) Delocalized excitation and excitation transfer. In Sinanoglu O (ed.), *Modern Quantum Chemistry: Instanbul Lectures. Part III. Action of Light and Organic Crystals*. New York: Academic, pp. 93–137.

Frauenfelder H and Wolynes PG (1985) Rate theories and puzzles of heme-protein kinetics. *Science* **229**, 337–345.

Fresch E, **Camargo F**, **Shen Q**, **Bellora C**, **Pullerits T**, **Engel GS**, **Cerullo G and Collini E** (2023) Two-dimensional electronic spectroscopy. *Nature Reviews Methods Primers* **3**, 84.

Fuller FD, **Pan J**, **Gelzinis A**, **Butkus V**, **Senlik SS**, **Wilcox DE**, **Yocum CF**, **Valkunas L**, **Abramavicius D and Ogilvie JP** (2014) Vibronic coherence in oxygenic photosynthesis. *Nature Chemistry* **6**(8), 706–711. https://doi.org/10.1038/nchem.2005.

Gallagher SM, **Albrecht AW**, **Hybl TD**, **Landin BL**, **Rajaram B and Jonas DM** (1998) Heterodyne detection of the complete electric field of femtosecond four-wave mixing signals. *Journal of the Optical Society of America B* **15**(8), 2338–2345.

Gaynor JD, **Weakly RB and Khalil M** (2021) Multimode two-dimensional vibronic spectroscopy. I. Orientational response and polarization-selectivity. *Journal of Chemical Physics* **154**, 184201.

Hamm P, **Lim M and Hochstrasser RM** (1998) Structure of the amide I band of peptides measured by femtosecond nonlinear-infrared spectroscopy. *Journal of Physical Chemistry B* **102**, 6123–6138.

Hayes D and Engel GS (2011) Extracting the excitonic Hamiltonian of the Fenna–Matthews–Olson complex using three-dimensional third-order electronic spectroscopy. *Biophysics Journal* **100**, 2043–2052.

Hayes D and Engel GS (2012) Peak shape analysis of diagonal and off-diagonal features in the two-dimensional electronic spectra of the Fenna–Matthews–Olson complex. *Philosophical Transactions of the Royal Society of London Series A* **370**, 3692–3708.

Hestand N and Spano FC (2018) Expanded theory of H- and J-molecular aggregates: The effects of vibronic coupling and intermolecular charge transfer. *Chemical Reviews* **118**, 7069–7163.

Higgins JS, **Lloyd LT**, **Sohail SH**, **Allodi MA**, **Otto JP**, **Saer RG**, **Wood RE**, **Massey SC**, **Ting PC**, **Blankenship RE and Engel GS** (2021) Photosynthesis tunes quantum-mechanical mixing of electronic and vibrational states to steer exciton energy transfer. *Proceedings of the National Academy of Sciences of the United States of America* **118**(11), e2018240118. https://doi.org/10.1073/pnas.2018240118.

Hochstrasser RM (2007) Two-dimensional spectroscopy at infrared and optical frequencies. *Proceedings of the National Academy of Sciences of the United States of America* **104**, 14190–14196.

Holdaway DIH, **Notararigo V and Olaya-Castro A** (2018) Perturbation approach for computing frequency- and time-resolved photon correlation functions. *Physical Reviews A* **98**, 063828.

Hossein-Nejad H, **Olaya-Castro A and Scholes GD** (2012) Phonon-mediated path-interference in electronic energy transfer *Journal of Chemical Physics* **136**, 024112.

Ishizaki A and Fleming GR (2009a) On the adequacy of the Redfield equation and related approaches to the study of quantum dynamics in electronic energy transfer. *Journal of Chemical Physics* **130**, 234110.

Ishizaki A and Fleming GR (2009b) Unified treatment of quantum coherent and incoherent hopping dynamics in electronic energy transfer: Reduced hierarchy equation approach. *Journal of Chemical Physics* **130**, 234111.

Ishizaki A and Fleming GR (2012) Quantum coherence in photosynthetic light harvesting. *Annual Reviews of Condensed Matter Physics* **3**, 333–361.

Jana S, **Do TN**, **Nowakowski PJ**, **Khyasudeen MF**, **Le DV**, **Lim IJY**, **Prasad S**, **Zhang JJ and Tan HS** (2023) Measuring the ultrafast correlation dynamics of a multilevel system using the center line slope analysis in two-dimensional electronic spectroscopy. *Journal of Physical Chemistry B* **127**, 7309–7322. https://doi.org/10.1021/acs.jpcb.3c02521.

Jang S (2011) Theory of multichromophoric coherent resonance energy transfer: A polaronic quantum master equation approach. *Journal of Chemical Physics* **135**, 034105.

Jang S and Cheng YC (2013) Resonance energy flow dynamics of coherently delocalized excitons in biological and macromolecular systems: Recent theoretical advances and open issues. *WIREs Computational Molecular Science* **3**, 84–104.

Jang S and Mennucci B (2018) Delocalized excitons in natural light-harvesting complexes. *Reviews of Modern Physics* **90**, 035003.

Jang S, **Newton M and Silbey R** (2004) Multichromophoric Forster resonance energy transfer. *Physical Review Letters* **92**, 218301.

Jeffries WR, **Aikens CM and Jr KLK** (2023) Symmetry-dependent dynamics in Au_{38} $(SC_6H_{13})_{24}$ revealed by polarization-dependent two-dimensional electronic spectroscopy. *Journal of Physical Chemistry C* **127**(38), 19035–19043. https://doi.org/10.1021/acs.jpcc.3c04832.

Jimenez R, **van Mourik F**, **Yu J and Fleming G** (1997) Three-pulse photon echo measurements on LH1 and LH2 complexes of *Rhodobacter sphaeroides*: A nonlinear spectroscopic probe of energy transfer. *Journal of Physical Chemistry B* **101**, 7350–7359.

Jonas DM (2003a) Optical analogs of 2D NMR. *Science* **300**, 1515–1517.

Jonas DM (2003b) Two-dimensional femtosecond spectroscopy. *Annual Reviews of Physical Chemistry* **54**, 425–463.

Joo T, **Jia Y**, **Ju J**, **Jonas DM and Fleming GR** (1996) Dynamics in isolated bacterial light harvesting antenna (LH2) of Rhodobacter sphaeroides at room temperature. *Journal of Physical Chemistry* **100**, 2399–2409.

Jordanides X, **Scholes G and Fleming G** (2001) The mechanism of energy transfer in the bacterial photosynthetic reaction center *Journal of Physical Chemistry B* **105**, 1652–1669.

Jun SH, **Yang C**, **Choi S**, **Isaji M**, **Tamiaki H**, **Ihee H and Kim J** (2021) Exciton delocalization length in chlorosomes investigated by lineshape dynamics of two-dimensional electronic spectra. *Physical Chemistry Chemical Physics* **23** (42), 24111–24117. https://doi.org/10.1039/d1cp03413h.

Kenkre VM and Knox RS (1974) Generalized-master-equation theory of excitation transfer. *Physical Review B* **9**, 5279–5290.

Kim J, **Nguyen-Phan TC**, **Gardiner AT**, **Cogdell RJ**, **Scholes GD and Cho M** (2021) Low-frequency vibronic mixing modulates the excitation energy flow in bacterial light-harvesting complex II. *Journal of Physical Chemistry Letters* **12**(27), 6292–6298. https://doi.org/10.1021/acs.jpclett.1c01782.

Kim J, **Nguyen-Phan TC**, **Gardiner AT**, **Yoon TH**, **Cogdell RJ**, **Cho M and Scholes GD** (2022a) Vibrational modes promoting exciton relaxation in the B850 band of LH2. *Journal of Physical Chemistry Letters* **13**(4), 1099–1106. https://doi.org/10.1021/acs.jpclett.1c03868.

Kim T, **Lin CJ**, **Schultz JD**, **Young RM and Wasielewski MR** (2022b) π-Stacking-dependent vibronic couplings drive excited-state in assemblies. *Journal of the American Chemical Society* **144**(25), 11386–11396. https://doi.org/10.1021/jacs.2c03993.

Kimura A and Kakitani T (2003) Theory of excitation energy transfer in the intermediate coupling case of clusters. *Journal of Physical Chemistry B* **107**, 14486–14499.

Kimura A, **Kakitani T and Yamato T** (2000) Theory of excitation energy transfer in the intermediate coupling case. II. Criterion for intermediate coupling excitation energy transfer mechanism and application to the photosynthetic antenna system. *Journal of Physical Chemistry B* **104**, 9276–9287.

Koepke J, **Hu X**, **Muenke C**, **Schulten K and Michel H** (1996) The crystal structure of the light-harvesting complex II (B800-850) from *Rhodospirillum molischianum*. *Structure* **4**, 581–597.

Koolhaas M, **Frese R**, **Fowler G**, **Bibby T**, **Georgakopoulou S**, **van der Zwan G**, **Hunter C and van Grondelle R** (1998) Identification of the upper exciton component of the B850 bacteriochlorophylls of the LH2 antenna complex, using a B800-free mutant of *Rhodobacter sphaeroides*. *Biochemistry* **37**, 4693–4698.

Krueger BP, **Scholes GD and Fleming GR** (1998) Calculation of couplings and energy transfer pathways between the pigments of LH2 by the ab initio transition density cube method. *Journal of Physical Chemistry B* **102**, 5378–5386.

Kühn O and Sundström V (1997) Pump-probe spectroscopy of dissipative energy transfer dynamics in photosynthetic antenna complexes: A density matrix approach. *Journal of Chemical Physics* **107**, 4154–4164.

Lee A, **Son M**, **Deegbey M**, **Woodhouse MD**, **Hart SM**, **Beissel HF**, **Cesana PT**, **Jakubikova E**, **McCusker JK and Schlau-Cohen GS** (2023) Observation of parallel intersystem crossing and charge transfer-state dynamics in Fe(bpy)$_3^{2+}$ from ultrafast 2D electronic spectroscopy. *Chemical Science* **14**(45), 13140–13150. https://doi.org/10.1039/d3sc02613b.

Lee Y, **Gorka M**, **Golbeck JH and Anna JM** (2018) Ultrafast energy transfer involving the red chlorophylls of cyanobacterial photosystem I probed through two-dimensional electronic spectroscopy. *Journal of the American Chemical Society* **140**(37), 11631–11638. https://doi.org/10.1021/jacs.8b04593.

Leegwater J (1996) Coherent versus incoherent energy transfer and trapping in photosynthetic antenna complexes. *Journal of Physical Chemistry* **100**, 14403–14409.

Leonardo C, **Yang S**, **Orcutt K**, **Iwai M**, **Arsenault EA and Fleming GR** (2024) Bidirectional energy flow in the photosystem II supercomplex. *The Journal of*

Physical Chemistry B **128**(33), 7941–7953. https://doi.org/10.1101/2023.1111.1130.569278.

Lewis KLM and Ogilvie JP (2012) Probing photosynthetic energy and charge transfer with two-dimensional electronic spectroscopy. *Journal of Physical Chemistry Letters* **3**(4), 503–510. https://doi.org/10.1021/jz201592v.

Lewis NHC, Dong H, Oliver TAA and Fleming GR (2015) A method for the direct measurement of electronic site populations in a molecular aggregate using two-dimensional electronic-vibrational spectroscopy. *Journal of Chemical Physics* **143**(12), 124203. https://doi.org/10.1063/1.4931634.

Lewis NHC, Gruenke NL, Oliver TAA, Ballottari M, Bassi R and Fleming GR (2016) Observation of electronic excitation transfer through light harvesting complex II using two-dimensional electronic-vibrational spectroscopy. *Journal of Physical Chemistry Letters* **7**, 4197–4206. https://doi.org/10.1021/acs.jpclett.6b02280.

Li XM, Buda F, de Groot HJM and Sevink GJA (2020) Dynamic disorder drives exciton transfer in tubular chlorosomal assemblies. *Journal of Physical Chemistry B* **124**(20), 4026–4035. https://doi.org/10.1021/acs.jpcb.0c00441.

Liu ZH, Jha A, Liang XT and Duan HG (2023) Transient chiral dynamics revealed by two-dimensional circular dichroism spectroscopy. *Physical Review E* **107**(5), 054119. https://doi.org/10.1103/PhysRevE.107.054119.

Lüttig J, Rose PA, Maly P, Turkin A, Bühler M, Lambert C, Krich JJ and Brixner T (2023) High-order pump-probe and high-order two-dimensional electronic spectroscopy on the example of squaraine oligomers. *Journal of Chemical Physics* **158**(23), 234201. https://doi.org/10.1063/5.0139090.

Ma F, Romero E, Jones MR, Novoderezhkin VI and van Grondelle R (2018) Vibronic coherence in the charge separation process of the *Rhodobacter sphaeroides* Reaction Center. *Journal of Physical Chemistry Letters* **9**(8), 1827–1832. https://doi.org/10.1021/acs.jpclett.8b00108.

Ma F, Romero E, Jones MR, Novoderezhkin VI and van Grondelle R (2019) Both electronic and vibrational coherences are involved in primary electron transfer in bacterial reaction center. *Nature Communications* **10**, 933. https://doi.org/10.1038/s41467-019-08751-8.

Ma F, Romero E, Jones MR, Novoderezhkin VI, Yu LJ and van Grondelle R (2022) Dynamics of diverse coherences in primary charge separation of bacterial reaction center at 77 K revealed by wavelet analysis. *Photosynthesis Research* **151**(3), 225–234. https://doi.org/10.1007/s11120-021-00881-9.

Ma F, Yu LJ, Hendrikx R, Wang-Otomo ZY and van Grondelle R (2017) Direct observation of energy detrapping in LH1-RC complex by two-dimensional electronic spectroscopy. *Journal of the American Chemical Society* **139**(2), 591–594. https://doi.org/10.1021/jacs.6b11017.

Madjet M, Abdurahman A and Renger T (2006) Intermolecular Coulomb couplings from ab initio electrostatic potentials: Application to optical transitions of strongly coupled pigments in photosynthetic antennae and reaction centers. *Journal of Physical Chemistry B* **110**, 17268–17281.

Maiuri M, Ostroumov EE, Saer R, Blankenship RE and Scholes GD (2018) Coherent wavepackets in the Fenna–Matthews–Olson complex are robust to exciton-structure perturbations caused by mutagenesis. *Nature Chemistry* **10**, 177–183.

Malý P, Lüttig J, Rose P, Turkin A, Lambert C, Krich J and Brixner T (2023) Separating single- from multi-particle dynamics in nonlinear spectroscopy. *Nature* **616**, 280–287.

Mančal T, Nemeth A, Milota F, Lukeš V, Kauffmann HF and Sperling J (2010) Vibrational wave packet induced oscillations in two-dimensional electronic spectra. II. Theory. *Journal of Chemical Physics* **132**, 184515.

Marin A, Doust AB, Scholes GD, Wilk KE, Curmi PM, van Stokkum IH and van Grondelle R (2011) Flow of excitation energy in the cryptophyte light-harvesting antenna phycocyanin 645. *Biophysical Journal* **101**(4), 1004–1013. https://doi.org/10.1016/j.bpj.2011.07.012.

Massey SC, Ting PC, Yeh SH, Dahlberg PD, Sohail SH, Allodi MA, Martin EC, Kais S, Hunter CN and Engel GS (2019) Orientational dynamics of transition dipoles and exciton relaxation in LH2 from ultrafast two-dimensional anisotropy. *Journal of Physical Chemistry Letters* **10**(2), 270–277. https://doi.org/10.1021/acs.jpclett.8b03223.

Matthews B and Fenna R (1980) Structure of a green bacteriochlorophyll protein. *Accounts of Chemical Research* **13**, 309–317.

McDermott G, Prince SM, Freer AA, Hawthornthwaite-Lawless AM, Papiz MZ, Cogdell RJ and Isaacs NW (1995) Crystal structure of an integral membrane light-harvesting complex from photosynthetic bacteria. *Nature* **374**, 517–521.

Milota F, Sperling J, Nemeth A, Mancal T and Kauffmann HF (2009) Two-dimensional electronic spectroscopy of molecular excitons. *Accounts of Chemical Research* **42**(9), 1364–1374. https://doi.org/10.1021/ar800282e.

Mirkovic T, Ostroumov EE, Anna JM, van Grondelle R, Govindjee and Scholes GD (2017) Light absorption and energy transfer in the antenna complexes of photosynthetic organisms. *Chemical Reviews* **117**, 249–293.

Mohan TMN, Leslie CH, Sil S, Rose JB, Tilluck RW and Beck WF (2021) Broadband 2DES detection of vibrational coherence in the S_x state of canthaxanthin. *Journal of Chemical Physics* **155**(3), 035103. https://doi.org/10.1063/5.0055598.

Monshouwer R, Abrahamsson M, van Mourik F and van Grondelle R (1997) Superradiance and exciton delocalization in bacterial photosynthetic light-harvesting systems. *Journal of Physical Chemistry B* **101**, 7241–7248.

Mueller S, Lüttig J, Brenneis L, Oron D and Brixner T (2021) Observing multiexciton correlations in colloidal semiconductor quantum dots *via* multiple-quantum two-dimensional fluorescence spectroscopy. *ACS Nano* **15**(3), 4647–4657. https://doi.org/10.1021/acsnano.0c09080.

Mukamel S (1995) *Principles of Nonlinear Optical Spectroscopy*. New York: Oxford University Press.

Mukamel S (2000) Multidimensional femtosecond correlation spectroscopies of electronic and vibrational excitations. *Annual Review of Physical Chemistry* **51**, 691–729.

Myers JA, Lewis KLM, Fuller FD, Tekavec PF, Yocum CF and Ogilvie JP (2010) Two-dimensional electronic spectroscopy of the D1-D2-cyt b559 photosystem II reaction center complex. *Journal of Physical Chemistry Letters* **1**(19), 2774–2780. https://doi.org/10.1021/jz100972z.

Nation C, Notararigo V, Gestsson H, Sapienza L and Olaya-Castro A (2024) Two-colour photon correlations probe coherent vibronic contributions to electronic excitation transport under incoherent illumination. https://arxiv.org/abs/2403.00857.

Nemeth A, Milota F, Mančal T, Lukeš V, Hauer J, Kauffmann HF and Sperling J (2010) Vibrational Wave Packet Induced Oscillations in Two-Dimensional Electronic Spectra. I. Experiments. *Journal of Chemical Physics* **132**, 184514.

Nguyen HH, Song Y, Maret E, Silori Y, Willow R, Yocum CF and Ogilvie JP (2023a) Charge separation in the photosystem II reaction center resolved by multispectral two-dimensional electronic spectroscopy. *Science Advances* **9**, eade719.

Nguyen XT, Winte K, Timmer D, Rakita Y, Ceratti DR, Aharon S, Ramzan MS, Cocchi C, Lorke M, Jahnke F, Cahen D, Lienau C and De Sio A (2023b) Phonon-driven intra-exciton Rabi oscillations in $CsPbBr_3$ halide perovskites. *Nature Communications* **14**(1), 1047. https://doi.org/10.1038/s41467-023-36654-2.

Niedringhaus A, Policht VR, Sechrist R, Konar A, Laible PD, Bocian DF, Holten D, Kirmaier C and Ogilvie JP (2018) Primary processes in the bacterial reaction center probed by two-dimensional electronic spectroscopy. *Proceedings of the National Academy of Science U S A* **115**(14), 3563–3568. https://doi.org/10.1073/pnas.1721927115.

Novoderezhkin V and van Grondelle R (2010) Physical origins and models of energy transfer in photosynthetic light-harvesting. *Physical Chemistry Chemical Physics* **12**, 7352–7365.

Novoderezhkin VI, Palacios MA, van Amerongen H and van Grondelle R (2005) Excitation dynamics in the LHCII complex of higher plants:: Modeling based on the 2.72 Å crystal structure. *Journal of Physical Chemistry B* **109**(20), 10493–10504. https://doi.org/10.1021/jp044082f.

Ogilvie J and Kubarych KJ (2009) Multidimensional electronic and vibrational spectroscopy: An ultrafast probe of molecular relaxation and reaction dynamics. *Advances in Optics and Molecular Optical Physics* **57**, 249–321.

Oliver TAA, Lewis NHC and Fleming GR (2014) Correlating the motion of electrons and nuclei with two-dimensional electronic-vibrational spectroscopy. *Proceedings of the National Academy of Sciences of the United States of America* **111**, 10061–10066. https://doi.org/10.1073/pnas.1409207111.

Ostroumov EE, Mulvaney RM, Cogdell RJ and Scholes GD (2013) Broadband 2D electronic spectroscopy reveals a carotenoid dark state in purple bacteria. *Science* **340**(6128), 52–56. https://doi.org/10.1126/science.1230106.

Palato S, **Seiler H**, **Nijjar P**, **Prezhdo O** and **Kambhampati P** (2020) Atomic fluctuations in electronic materials revealed by dephasing. *Proceedings of the National Academy of Sciences of the United States of America* **117**(22), 11940–11946. https://doi.org/10.1073/pnas.1916792117.

Palecek D, **Edlund P**, **Gustavsson E**, **Westenhoff S** and **Zigmantas D** (2019) Potential pitfalls of the early-time dynamics in two-dimensional electronic spectroscopy. *Journal of Chemical Physics* **151**(2), 024201. https://doi.org/10.1063/1.5079817.

Panitchayangkoon G, **Hayes D**, **Fransted KA**, **Caram JR**, **Harel E**, **Wen JZ**, **Blankenship RE** and **Engel GS** (2010) Long-lived quantum coherence in photosynthetic complexes at physiological temperature. *Proceedings of the National Academy of Sciences of the United States of America* **107**(29), 12766–12770.

Perlík V, **Seibt J**, **Cranston LJ**, **Cogdell RJ**, **Lincoln CN**, **Savolainen J**, **Sanda F**, **Mancal T** and **Hauer J** (2015) Vibronic coupling explains the ultrafast carotenoid-to-bacteriochlorophyll energy transfer in natural and artificial light harvesters. *Journal of Chemical Physics* **142**(21), 212434. https://doi.org/10.1063/1.4919548.

Plenio MB, **Almeida J** and **Huelga SF** (2013) Origin of long-lived oscillations in 2D-spectra of a quantum vibronic model: Electronic versus vibrational coherence. *Journal of Chemical Physics* **139**, 235102.

Policht VR, **Niedringhaus A**, **Willow R**, **Laible PD**, **Bocian DF**, **Kirmaier C**, **Holten D**, **Mancal T** and **Ogilvie JP** (2022) Hidden vibronic and excitonic structure and vibronic coherence transfer in the bacterial reaction center. *Science Advances* **8**(1), eabk0953. https://doi.org/10.1126/sciadv.abk0953.

Polley K and **Loring R** (2022) 2D electronic-vibrational spectroscopy with classical trajectories. *Journal of Chemical Physics* **156**, 204110.

Pullerits T, **Chachisvilis M** and **Sundström V** (1996) Exciton delocalization length in the B850 antenna of *Rhodobacter sphaeroides*. *Journal of Physical Chemistry* **100**, 10787–10792.

Read EL, **Engel GS**, **Calhoun TR**, **Mancal T**, **Ahn TK**, **Blankenship RE** and **Fleming GR** (2007) Cross-peak-specific two-dimensional electronic spectroscopy. *Proceedings of the National Academy of Sciences of the United States of America* **104**(36), 14203–14208. https://doi.org/10.1073/pnas.0701201104.

Rebentrost P, **Mohseni M** and **Aspuru-Guzik A** (2009a) Role of quantum coherence and environmental fluctuations in chromophoric energy transport. *Journal of Physical Chemistry B* **113**, 9942–9947.

Rebentrost P, **Mohseni M**, **Kassal I**, **Lloyd S** and **Aspuru-Guzik A** (2009b) Environment-assisted quantum transport. *New Journal of Physics* **11**, 033003.

Reimers J, **McKemmish L**, **McKenzie R** and **Hush N** (2015) Non-adiabatic effects in thermochemistry, spectroscopy and kinetics: the general importance of all three Born–Oppenheimer breakdown corrections. *Physical Chemistry Chemical Physics* **17**, 24641–24665.

Reimers JR, **Cai Z**, **Kobayashi R**, **Ratsep M**, **Freiberg A** and **Krausz E** (2013) Assignment of the Q-bands of the chlorophylls: Coherence loss via Qx-Qy mixing. *Scientific Reports* **3**, 2761.

Renger T (2009) Theory of excitation energy transfer: from structure to function. *Photosynthesis Research* **102**, 471–485.

Renger T and **Müh F** (2012) Theory of excitonic couplings in dielectric media foundation of Poisson-TrEsp method and application to photosystem I trimers. *Photosynthesis Research* **111**, 47–52.

Robinson GW (1966) Excitation transfer and trapping in photosynthesis. *Brookhaven Symposium in Biology* **19**, 16.

Rojas-Gatjens E, **Li H**, **Vega-Flick A**, **Cortecchia D**, **Petrozza A**, **Bittner ER**, **Kandada ARS** and **Silva-Acuña C** (2023) Many-exciton quantum dynamics in a Ruddlesden–Popper tin iodide. *Journal of Physical Chemistry C* **127**(43), 21194–21203. https://doi.org/10.1021/acs.jpcc.3c04896.

Romero E, **Augulis R**, **Novoderezhkin VI**, **Ferretti M**, **Thieme J**, **Zigmatus D** and **van Grondelle R** (2014) Quantum coherence in photosynthesis for efficient solar-energy conversion. *Nature Physics* **10**, 677–683.

Roscioli JD, **Ghosh S**, **LaFountain AM**, **Frank HA** and **Beck WF** (2017) Quantum coherent excitation energy transfer by carotenoids in photosynthetic light harvesting. *Journal of Physical Chemistry Letters* **8**(20), 5141–5147. https://doi.org/10.1021/acs.jpclett.7b01791.

Roscioli JD, **Ghosh S**, **LaFountain AM**, **Frank HA** and **Beck WF** (2018) Structural tuning of quantum decoherence and coherent energy transfer in photosynthetic light harvesting. *Journal of Physical Chemistry Letters* **9**(17), 5071–5077. https://doi.org/10.1021/acs.jpclett.8b01919.

Ross AM, **Osella S**, **Policht VR**, **Zheng M**, **Maggini M**, **Marangi F**, **Cerullo G**, **Gatti T** and **Scotognella F** (2022) Deciphering photoinduced charge transfer dynamics in a cross-linked graphene-dye nanohybrid. *Journal of Physical Chemistry C* **126**(7), 3569–3581. https://doi.org/10.1021/acs.jpcc.1c10570.

Roy PP, **Kundu S**, **Valdiviezo J**, **Bullard G**, **Fletcher JT**, **Liu R**, **Yang S**, **Zhang P**, **Beratan DN**, **Therien MJ**, **Makri N** and **Fleming GR** (2022) Synthetic control of exciton dynamics in bioinspired cofacial porphyrin dimers. *Journal of the American Chemical Society* **144**(14), 6298–6310. https://doi.org/10.1021/jacs.1c12889.

Russo M, **Casazza AP**, **Cerullo G**, **Santabarbara S** and **Maiuri M** (2021) Direct evidence for excitation energy transfer limitations imposed by low-energy chlorophylls in photosystem I-light harvesting complex I of land plants. *Journal of Physical Chemistry B* **125**(14), 3566–3573. https://doi.org/10.1021/acs.jpcb.1c01498.

Sánchez Muñoz C and **Schlawin F** (2020) Photon correlation spectroscopy as a witness for quantum coherence. *Physical Review Letters* **124**, 203601.

Sardjan AS, **Westerman FP**, **Ogilvie JP** and **Jansen TLC** (2020) Observation of ultrafast coherence transfer and degenerate states with polarization-controlled two-dimensional electronic spectroscopy. *Journal of Physical Chemistry B* **124**(42), 9420–9427. https://doi.org/10.1021/acs.jpcb.0c08126.

Schlau-Cohen GS, **Calhoun TR**, **Ginsberg NS**, **Read EL**, **Ballottari M**, **Bassi R**, **van Grondelle R** and **Fleming GR** (2009) Pathways of energy flow in LHCII from two-dimensional electronic spectroscopy. *Journal of Physical Chemistry B* **113**, 15352–15363.

Schlau-Cohen GS, **Dawlaty JM** and **Fleming GR** (2012) Ultrafast multidimensional spectroscopy: Principles and applications to photosynthetic systems. *IEEE Journal of Selected Topics in Quantum Electronics* **18**, 283–295.

Scholes G (2020) Polaritons and excitons: Hamiltionian design for enhanced coherence. *Proceedings of the Royal Society A* **476**, 20200278.

Scholes GD (2003) Long-range resonance energy transfer in molecular systems. *Annual Review of Physical Chemistry* **54**, 57–87.

Scholes GD (2010) Quantum-coherent electronic energy transfer: Did nature think of it first? *Journal of Physical Chemistry Letters* **1**, 2–8.

Scholes GD, **Curutchet C**, **Mennucci B**, **Cammi R** and **Tomasi J** (2007) How solvent controls electronic energy transfer and light harvesting. *Journal of Physical Chemistry B* **111**, 6978–6982.

Scholes GD, **Fleming G**, **Chen L**, **Aspuru-Guzik A**, **Buchleitner A**, **Coker D**, **Engel G**, **van Grondelle R**, **Ishizaki A**, **Jonas D**, **Lundeen J**, **McCusker J**, **Mukamel S**, **Ogilvie J**, **Olaya-Castro A**, **Ratner M**, **Spano F**, **Whaley K** and **Zhu X** (2017) Utilizing coherence to enhance function in chemical and biophysical systems. *Nature* **543**, 647–656.

Scholes GD and **Fleming GR** (2000) On the mechanism of light-harvesting in photosynthetic purple bacteria: B800 to B850 energy transfer. *Journal of Physical Chemistry B* **104**, 1854–1868.

Scholes GD, **Fleming GR**, **Olaya-Castro A** and **van Grondelle R** (2011) Lessons from nature about solar light harvesting. *Nature Chemistry* **3**, 763–774.

Scholes GD, **Gould IR**, **Cogdell RJ** and **Fleming GR** (1999) *Ab initio* molecular orbital calculations of electronic couplings in the LH2 bacterial light-harvesting complex of *Rps. acidophila*. *Journal of Physical Chemistry B* **103**, 2543–2553.

Scholes GD, **Harcourt RD** and **Ghiggino KP** (1995) Rate expressions for excitation transfer. III. An ab initio study of electronic factors in excitation transfer and exciton resonance interactions. *Journal of Chemical Physics* **102**, 9574–9581.

Scholes GD, **Jordanides XJ** and **Fleming GR** (2001) Adapting the Förster theory of energy transfer for modeling dynamics in aggregated molecular assemblies. *Journal of Physical Chemistry B* **105**, 1640–1651.

Scholes GD, **Mirkovic T**, **Turner DB**, **Fassioli F** and **Buchleitner A** (2012) Solar light harvesting by energy transfer: From ecology to coherence. *Energy and Environmental Science* **5**, 9374–9393.

Schröter M, **Alcocer MJP**, **Cogdell RJ**, **Kühn O** and **Zigmantas D** (2018) Origin of the two bands in the B800 ring and their involvement in the energy transfer network of *Allochromatium vinosum*. *Journal of Physical Chemistry Letters* **9**(6), 1340–1345. https://doi.org/10.1021/acs.jpclett.8b00438.

Schultz JD, **Kim T**, **O'Connor JP**, **Young RM** and **Wasielewski MR** (2022) Coupling between harmonic vibrations influences quantum beating

signatures in two-dimensional electronic spectra. *Journal of Physical Chemistry C* **126**(1), 120–131. https://doi.org/10.1021/acs.jpcc.1c09432.

Segarra-Martí J, Segatta F, Mackenzie TA, Nenov A, Rivalta I, Bearpark MJ and Garavelli M (2020) Modeling multidimensional spectral lineshapes from first principles: application to water-solvated adenine. *Faraday Discussions* **221**, 219–244. https://doi.org/10.1039/c9fd00072k.

Sirohiwal A, Neese F and Pantazis DA (2020) Protein matrix control of reaction center excitation in photosystem II. *Journal of the American Chemical Society* **142**(42), 18174–18190. https://doi.org/10.1021/jacs.0c08526.

Sirohiwal A and Pantazis DA (2023) Reaction center excitation in photosystem II: From multiscale modeling to functional principles. *Accounts of Chemical Research* **56**(21), 2921–2932. https://doi.org/10.1021/acs.accounts.3c00392.

Son M, Hart SM and Schlau-Cohen GS (2021) Investigating carotenoid photophysics in photosynthesis with 2D electronic spectroscopy. *Trends in Chemistry* **3**(9), 733–746. https://doi.org/10.1016/j.trechm.2021.05.008.

Son MJ, Pinnola A, Gordon SC, Bassi R and Schlau-Cohen GS (2020a) Observation of dissipative chlorophyll-to-carotenoid energy transfer in light-harvesting complex II in membrane nanodiscs. *Nature Communications* **11**(1), 1295. https://doi.org/10.1038/s41467-020-15074-6.

Son MJ, Pinnola A and Schlau-Cohen GS (2020b) Zeaxanthin independence of photophysics in light-harvesting complex II in a membrane environment. *Biochimica et Biophysica Acta-Bioenergetics* **1861**(5–6), 148115. https://doi.org/10.1016/j.bbabio.2019.148115.

Song Y, Liu X, Li Y, Nguyen HH, Duan R, Kubarych KJ, Forrest SR, and Ogilvie JP (2021a) Mechanistic study of charge separation in a nonfullerene organic donor-acceptor blend using multispectral multidimensional spectroscopy. *Journal of Physical Chemistry Letters* **12**, 3410–3416.

Song Y, Schubert A, Maret E, Burdick RK, Dunietz BD, Geva E and Ogilvie JP (2019) Vibronic structure of photosynthetic pigments probed by polarized two-dimensional electronic spectroscopy and *ab initio* calculations. *Chemical Science* **10**(35), 8143–8153. https://doi.org/10.1039/c9sc02329a.

Song Y, Sechrist R, Nguyen HH, Johnson W, Abramavicius D, Redding KE and Ogilvie JP (2021b) Excitonic structure and charge separation in the heliobacterial reaction center probed by multispectral multidimensional spectroscopy. *Nature Communications* **12**(1), 2801. https://doi.org/10.1038/s41467-021-23060-9.

Sturgis J, Tucker J, Olsen J, Hunter C and Niederman R (2009) Atomic force microscopy studies of native photosynthetic membranes. *Biochemistry* **48**, 3679–3698.

Sumi H (1999) Theory on rates of excitation-energy transfer between molecular aggregates through distributed transition dipoles with application to the antenna system in bacterial photosynthesis *Journal of Physical Chemistry B* **103**, 252–260.

Sundström V, van Grondelle R and Gillbro T (1986) Excitation-energy transport in the bacteriochlorophyll antenna systems of *Rhodospirillum rubrum* and *Rhodobacter sphaeroides*, studied by low-intensity picosecond absorption spectroscopy. *Biochimica Biophysica Acta* **851**, 431–446.

Szalay L, Tombácz E and Singhal GS (1974) Effect of solvent on the absorption spectra and Stokes' shift of absorption and fluorescence of chlorophylls. *Acta Physica Hungaricae* **35**, 29–36.

Tanimura Y (2006) Stochastic Lionville, Langevin, Fokker-Planck, and master equation approaches to quantum dissipative systems. *Journal of the Physical Society of Japan* **75**, 082001.

Tanimura Y and Mukamel S (1993) 2-dimensional femtosecond vibrational spectroscopy of liquids. *Journal of Chemical Physics* **99**, 9496–9511.

Thyrhaug E, Schröter M, Bukarte E, Kühn O, Cogdell R, Hauer J and Zigmantas D (2021) Intraband dynamics and exciton trapping in the LH2 complex of *Rhodopseudomonas acidophila*. *Journal of Chemical Physics* **154**(4), 045102. https://doi.org/10.1063/5.0033802.

Thyrhaug E, Tempelaar R, Alcocer M, Zidek K, Bina D, Knoester J, Jansen TLC and Zigmantas D (2018) Identification and characterization of diverse coherences in the Fenna–Matthews–Olson complex. *Nature Chemistry* **10**, 780–786.

Thyrhaug E, Zídek K, Dostál J, Bína D and Zigmantas D (2016) Exciton structure and energy transfer in the Fenna–Matthews–Olson complex. *Journal of Physical Chemistry Letters* **7**(9), 1653–1660. https://doi.org/10.1021/acs.jpclett.6b00534.

Tilluck RW, Ghosh S, Guberman-Pfeffer MJ, Roscioli JD, Gurchiek JK, LaFountain AM, Frank HA, Gascón JA and Beck WF (2021) Interexciton nonradiative relaxation pathways in the peridinin-chlorophyll protein. *Cell Reports Physical Science* **2**(3), 100380. https://doi.org/10.1016/j.xcrp.2021.100380.

Timmer D, Zheng FL, Gittinger M, Quenzel T, Lünemann DC, Winte K, Zhang Y, Madjet ME, Zablocki J, Lützen A, Zhong JH, De Sio A, Frauenheim T, Tretiak S and Lienau C (2022) Charge delocalization and vibronic couplings in quadrupolar squaraine dyes. *Journal of the American Chemical Society* **144**, 19150–19162. https://doi.org/10.1021/jacs.2c08682.

Tiwari V, Peters WK and Jonas DM (2013) Electronic resonance with anticorrelated pigment vibrations drives photosynthetic energy transfer outside the adiabatic framework. *Proceedings of the National Academy of Science USA* **110**, 1203–1208.

Toa ZSD, deGolian MH, Jumper CC, Hiller RG and Scholes GD (2019) Consistent model of ultrafast energy transfer in peridinin chlorophyll-*a* protein using two-dimensional electronic spectroscopy and Forster theory. *Journal of Physical Chemistry B* **123**(30), 6410–6420. https://doi.org/10.1021/acs.jpcb.9b04324.

Tran NL, Elkins MH, McMeekin DP, Snaith HJ and Scholes GD (2020) Observation of charge generation via photoinduced stark effect in mixed-cation lead bromide perovskite thin films. *Journal of Physical Chemistry Letters* **11**(23), 10081–10087. https://doi.org/10.1021/acs.jpclett.0c03044.

Tros M, Novoderezhkin VI, Croce R, van Grondelle R and Romero E (2020) Complete mapping of energy transfer pathways in the plant light-harvesting complex Lhca4. *Physical Chemistry Chemical Physics* **22**(44), 25720–25729. https://doi.org/10.1039/d0cp03351k.

Tumbarello F, Marcolin G, Fresch E, Hofmann E, Carbonera D and Collini E (2022) The energy transfer yield between carotenoids and chlorophylls in peridinin chlorophyll *a* protein is robust against mutations. *International Journal of Molecular Sciences* **23**(9), 5067. https://doi.org/10.3390/ijms23095067.

Turner DB, Dinshaw R, Lee KK, Belsley MS, Wilk KE, Curmi PM and Scholes GD (2012) Quantitative investigations of quantum coherence for a light-harvesting protein at conditions simulating photosynthesis. *Physical Chemistry Chemical Physics* **14**(14), 4857–4874. https://doi.org/10.1039/c2cp23670b.

Turner DB, Wilk KE, Curmi PMG and Scholes GD (2011) Comparison of electronic and vibrational coherence measured by two-dimensional electronic spectroscopy. *Journal of Physical Chemistry Letters* **2**, 1904–1911.

Walla PJ, Linden P, Hsu C, Scholes GD and Fleming GR (2000) Femtosecond dynamics of the forbidden carotenoid S1 state in light-harvesting complexes of purple bacteria observed after two-photon excitation. *Proceedings of the National Academy of Science USA* **97**, 10808–10813.

Wang L, Allodi M and Engel G (2019) Quantum coherences reveal excited-state dynamics in biophysical systems. *Nature Reviews Chemistry* **3**, 477–490.

Weakly RB, Gaynor JD and Khalil M (2021) Multimode two-dimensional vibronic spectroscopy. II. Simulating and extracting vibronic coupling parameters from polarization-selective spectra. *Journal of Chemical Physics* **154**, 184202.

Westenhoff S, Palecek D, Edlund P, Smith P and Zigniantas D (2012) Coherent picosecond exciton dynamics in a photosynthetic reaction center. *Journal of the American Chemical Society* **134**(40), 16484–16487. https://doi.org/10.1021/ja3065478.

Wolynes PG (1987) Dissipation, tunneling, and adiabaticity criteria for curve crossing problems in the condensed phase. *Journal of Chemical Physics* **86**, 1957–1966.

Wong CY, Alvey RM, Turner DB, Wilk KE, Bryant DA, Curmi PMG, Silbey RJ and Scholes GD (2012) Electronic coherence lineshapes reveal hidden excitonic correlations in photosynthetic light harvesting. *Nature Chemistry* **4**, 396–404.

Wu H, Ratsep M, Lee I, Cogdell R and Small G (1997) Exciton level structure and energy disorder of the B850 ring and the LH2 antennal complex. *Journal of Physical Chemistry B* **101**, 7654–7663.

Yang M and Fleming GR (2002) Influence of phonons on exciton transfer dynamics: comparison of Redfield, Förster, and modified Redfield equations. *Chemical Physics* **275**, 355.

Yang S-J, Wales D, Woods E and Fleming GR (2024) Design principles for energy transfer in the photosystem II supercomplex from kinetic transition

networks. *Nature Communications.* https://doi.org/10.1038/s41467-024-53138-z

Yang SJ, Arsenault EA, Orcutt K, Iwai M, Yoneda Y and Fleming GR (2022) From antenna to reaction center: Pathways of ultrafast energy and charge transfer in photosystem II. *Proceedings of the National Academy of Science U S A* **119**(42). https://doi.org/10.1073/pnas.2208033119.

Yoneda Y, Arsenault EA, Yang S, Orcutt K, Iwai M and Fleming GR (2022) The initial charge separation step in oxygenic photosynthesis. *Nature Communications* **13**(1), 2275. https://doi.org/10.1038/s41467-022-29983-1.

Zhang WM, Meier T, Chernyak V and Mukamel S (1998) Exciton-migration and three-pulse femtosecond optical spectroscopies of photosynthetic antenna complexes. *Journal of Chemical Physics* **108**(18), 7763–7774. https://doi.org/10.1063/1.476212.

Zhang X, Liu Z, Jha A, Liang X-T, Thorwart M, Miller R and Duan H-G (2023) Disentangling the complexity of coupled vibrations by two-dimensional electronic-vibrational spectroscopy. *Journal of Physics B: Atomic, Molecular and Optical Physics* **56**, 145001.

Zhao XG, O'Connor JP, Schultz JD, Bae YJ, Lin CJ, Young RM and Wasielewski MR (2021) Temperature tuning of coherent mixing between states driving singlet fission in a spiro-fused terrylenediimide dimer. *Journal of Physical Chemistry B* **125**(25), 6945–6954. https://doi.org/10.1021/acs.jpcb.1c02476.

Zigmantas D, Read EL, Mancal T, Brixner T, Gardiner AT, Cogdell RJ and Fleming GR (2006) Two-dimensional electronic spectroscopy of the B800-B820 light-harvesting complex. *Proceedings of the National Academy of Science U S A* **103**(34), 12672–12677. https://doi.org/10.1073/pnas.0602961103.

Zuehlsdorff TJ, Hong HB, Shi L and Isborn CM (2020) Nonlinear spectroscopy in the condensed phase: The role of Duschinsky rotations and third order cumulant contributions. *Journal of Chemical Physics* **153**(4), 044127. https://doi.org/10.1063/5.0013739.